Nano Research Energy

ISSN 2791-0091 (print); 2790-8119 (online)
https://doi.org/10.26599/NRE.2026.9120222

Review Article

Integrated design of wearable aqueous zinc-ion batteries: From energy autonomy to intelligent sensing

Wei Lv (✉), Junlin Liu, Zilei Shen, Qiumei Li, Xinming Wei, and Chao Xu (✉)

Beijing Laboratory of New Energy Storage Technology, Institute of Energy Power Innovation, North China Electric Power University, Beijing 102206, China

Received: 19 January 2026 / **Revised:** 9 February 2026 / **Accepted:** 21 February 2026 / **Published date:** 20 March 2026

ABSTRACT

With the advancement of wearable electronics toward longer battery life, multifunctionality, and intelligence, traditional rigid energy storage devices and discrete modules for energy harvesting, storage, and sensing are increasingly inadequate in meeting the demands of wearable systems for flexibility, safety, integration, and self-powering capabilities. Aqueous zinc-ion batteries (AZIBs) have emerged as an ideal candidate for constructing wearable energy systems due to their intrinsic safety, low cost, environmental friendliness, and excellent electrochemical performance. This review focuses on integrated systems of wearable AZIBs, systematically elaborating their development pathway from achieving "energy autonomy" to enabling "intelligent sensing". First, the fundamental principles, advantages, and necessity of integrated technologies for wearable AZIBs are analyzed. Next, recent research advancements in this field are comprehensively reviewed. Finally, current key challenges are summarized, and prospects for the future development of truly self-driven, intelligent, and comfortable wearable AZIBs systems are discussed.

KEYWORDS

aqueous zinc-ion batteries, wearable electronics, integrated system, mechanisms, energy storage

1 Introduction

With the rapid development of wearable electronics, flexible, safe, and sustainable energy supply has become a key bottleneck limiting their widespread application [1–8]. Traditional rigid energy storage devices struggle to meet the requirements of wearable devices for lightweight design, deformability, and biocompatibility, while reliance on external charging also restricts device autonomy [9–17]. Under this background, wearable aqueous zinc-ion batteries (AZIBs), with their inherent safety, environmental friendliness, and good electrochemical performance, have emerged as a reliable foundation for constructing smart wearable systems [18–20].

By integrating functions such as energy harvesting (e.g., from solar cells, triboelectric nanogenerators), conversion, and storage, wearable AZIB systems could continuously harvest energy from multi-source environmental inputs like light and human motion without the need for an external power supply [21–25]. They enable stable energy storage and on-demand release, thereby overcoming the limitations of traditional batteries, such as short endurance and frequent recharging [26–31]. This significantly enhances energy autonomy, convenience, and environmental adaptability of wearable devices [32–38]. Furthermore, wearable AZIB sensing systems achieve deep integration of power supply and perception through a multi-coupling mechanism of mechanical-electrochemical-signal interactions [39–44]. The electrochemical response signals generated by AZIBs under external mechanical stimuli can serve as an auxiliary sensing source, forming a dual-channel signal synergy with independent sensors [45–52]. AZIBs thus fulfill both energy supply and auxiliary sensing functions, while sensor structure could also act as mechanical support or an ionic interface for AZIBs [53–55]. This completes a closed-loop conversion from mechanical energy to chemical energy, electrical energy, and information flow, providing a key technological pathway for wearable devices to achieve long-term, stable, and intelligent sensing in dynamic environments [56–59]. It also improves system monitoring accuracy and enables self-calibration functions [60–66]. Wearable AZIBs demonstrate diverse technological pathways, encompassing multi-mechanism coupling systems involving light, electrochemistry, and mechanics. However, the development of this field remains constrained by key challenges such as flexible structural design, multi-physics field coordination, and energy-signal integration [67–70]. Furthermore, related research about wearable AZIBs is relatively fragmented and urgently requires systematic summarization and organization [71–74].

This review adopts a dual perspective of energy storage and energy sensing, comprehensively summarizing the current research progress in wearable AZIB systems. By systematically

Address correspondence to Wei Lv, luidavid@126.com; Chao Xu, mechxu@ncepu.edu.cn

explaining working principles of such systems, we focus on analyzing their structural design strategies and multi-physics coupling mechanisms, thereby clarifying the necessity and advantages of system integration. Drawing on representative studies from recent years, this article systematically explores construction methods of different integrated wearable AZIB systems. Finally, we identify main challenges in the field and offer an outlook on future development directions, aiming to provide theoretical reference and technical guidance for advancing wearable AZIB intelligent systems (Fig. 1).

2 Fundamentals of integrated wearable AZIBs

By constructing a multimodal energy-information synergistic system based on wearable AZIBs, functional integration and self-powered operation of wearable devices can be achieved. Meanwhile, key challenges must be addressed, including dynamic matching of energy and signals under multi-physics coupling, long-term stable maintenance of flexible heterogeneous interfaces under repeated deformation and environmental interference, as well as system-level optimization of energy harvesting, storage, conversion, and information processing within limited space available for wearables [75–77]. Through multi-dimensional collaborative design spanning structure, materials, circuits, and algorithms, wearable AZIB integration technology can be advanced towards intelligent forms characterized by efficient self-powering, high integration density, and strong environmental adaptability (Fig. 2).

2.1 Operating principle

2.1.1 *Solar plus storage*

The integrated energy system combining wearable AZIBs and solar cells operates on the principle of establishing a closed-loop energy cycle that synergizes the conversion and intelligent management of light, electrical, and chemical energy [78–81]. This enables a self-sustaining cycle from environmental energy harvesting to stable power supply. The process begins with solar cells converting ambient light energy into electricity via photovoltaic effect. Subsequently, an efficient power management circuit acts as the system's "intelligent hub", performing precise electrical energy regulation. It optimizes energy harvesting efficiency of solar cells through maximum power point tracking technology and executes accurate voltage conversion and current regulation to ensure that the output electricity matches charging requirements of the subsequent AZIB energy storage unit. The stabilized electrical energy then drives reversible electrochemical reactions, efficiently and safely storing electrical energy in the form of chemical energy in AZIBs.

2.1.2 *Integrated triboelectric nanogenerator*

The integrated system combining AZIBs with triboelectric nanogenerators operates based on a multistage conversion and dynamic synergistic management mechanism that transforms mechanical energy into electrical energy and ultimately into chemical energy. This is achieved by efficiently capturing low-frequency, irregular mechanical energy from daily human motion or the environment (such as vibration, friction, and pressure) and converting it into high-voltage, intermittent pulsed electrical energy [82–85]. The dedicated power management circuit integrated into the system first rectifies pulsed alternating current into direct current. It then regulates, stabilizes, and optimizes the current to transform it into stable direct current electricity that meets the efficient and safe charging requirements of AZIBs. Finally, the conditioned electrical energy drives reversible electrochemical reactions within AZIBs, enabling stable storage of electrical energy in the form of chemical energy. This entire process achieves real-time, efficient coupling between the harvesting of transient, disordered mechanical energy and stable, ordered electrochemical energy storage.

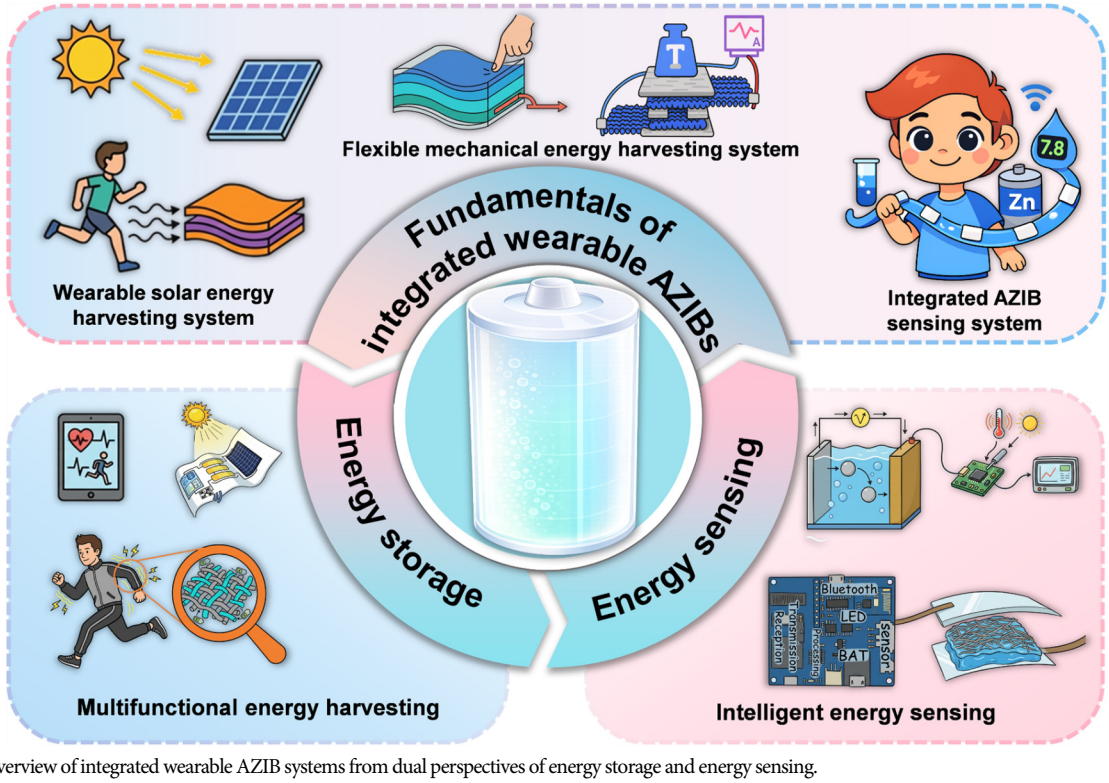

Figure 1 Overview of integrated wearable AZIB systems from dual perspectives of energy storage and energy sensing.

Figure 2 Operating principles and advantages of integrated wearable AZIB systems.

2.1.3 *Intelligent energy supply & perception*

The integrated system of wearable AZIBs with sensors achieves unified operation of energy supply and sensing through a multi-coupling mechanism involving mechanical force, electrochemistry, and signals. When the system is subjected to external mechanical actions (such as pressure, bending, or vibration), characteristic electrical signals directly correlated with mechanical input (such as voltage fluctuations, impedance responses, or transient currents) are generated within AZIBs due to changes in electrode/electrolyte interface structure and disturbances in ion transport dynamics [83–87]. Simultaneously, integrated sensor converts the same mechanical signal into an independent electrical signal through deformation of its sensitive structure. The self-generated mechanical-electrochemical coupling signals of AZIBs and mechanical-electric conversion signals output by sensor are synchronously collected and input into a signal processing module for comparison and decoupling analysis, thereby enhancing the accuracy and anti-interference capability of mechanical perception. AZIBs not only serve as an energy storage unit to continuously power the sensor and circuits but also act as auxiliary sensing unit by capturing mechanical signals. Meanwhile, the sensor, while performing signal detection, can also utilize its structural layers as mechanical support or ionic transport interfaces for AZIBs.

2.2 Advantage and necessity

Flexible integrated AZIB systems maintain structural integrity and functional stability even under dynamic bending, stretching, and humid environments. Through compact structural integration, they efficiently coordinate energy harvesting, storage, and output within the limited space available for wearables, significantly improving spatial and energy utilization efficiency while ensuring lightweight design and wearing comfort. The non-flammable nature of aqueous electrolytes guarantees the intrinsic safety of the system.

By efficiently capturing and converting ambient light energy through solar cells, a continuous energy supply loop of "light-electrical-chemical" energy is established. The integrated system of wearable AZIBs and solar cells substantially extends device endurance, reduces reliance on traditional grid charging, and overcomes power supply interruptions of single energy storage units in scenarios with no light, low light, or high power consumption [88–91]. Similarly, integrated system of wearable AZIBs and triboelectric nanogenerators efficiently captures mechanical energy from human motion and the environment and converts it into electrical energy, which is then stably stored by AZIBs. This forms a continuous conversion and closed-loop energy supply system of "mechanical-electrical-chemical" energy [92–95]. This approach directly addresses the core challenge of frequent recharging or replacement of traditional batteries in dynamic wearable scenarios, significantly enhancing the energy autonomy and endurance of wearable devices.

The integrated system of wearable AZIBs and sensors employs an energy storage-perception unified structure, enabling AZIBs to provide continuous electrical power while directly converting external mechanical stimuli (such as pressure, deformation, or vibration) into real-time response signals reflecting its internal electrochemical state [96–100]. These signals form a dual-channel synergistic perception mechanism alongside the independent mechanical signals captured by the sensor, significantly enhancing detection sensitivity, anti-interference capability, and signal reliability. This achieves efficient unification of energy supply and information acquisition within a limited volume [101–103]. Furthermore, the integrated system utilizes its self-generated battery signals to enable autonomous calibration of sensor drift and adaptive environmental compensation. This provides a self-powered, high-precision, and highly reliable intelligent perception solution for applications such as health monitoring, motion analysis, and human-computer interaction, driving wearable devices toward greater lightweight design, intelligence, and functional integration.

3 Energy storage

The integration of AZIBs with environmental energy harvesting

units to construct self-powered energy systems is of paramount significance. Such integrated systems enable real-time conversion of widely available but dispersed and intermittent environmental energy into electricity, which is then stored in highly safe AZIBs. This achieves *in-situ* energy harvesting, storage, and on-demand supply, thereby eliminating reliance on external power sources and providing a continuous, stable, and self-sustaining energy solution for wearable devices.

3.1 Yarn and fiber electrodes for photovoltaic integration

A central structural challenge in constructing solar-integrated AZIB systems lies in reconciling the geometric and mechanical mismatches between deformable storage units and photovoltaic elements embedded in textiles. Fiber-shaped AZIBs, with their one-dimensional geometry, high aspect ratio, and textile-processable form factor, provide a mechanically compliant and geometrically continuous platform for integration [104]. The internal architecture of fiber electrodes, including the spatial arrangement of current-collecting networks, active material distribution, and ion-transport pathways, determines how effectively the electrode accommodates the low-rate, intermittent charging conditions characteristic of photovoltaic inputs. Such structural tunability is essential for achieving stable charge acceptance under fluctuating irradiance and maintaining robust energy-harvesting-storage coupling during continuous mechanical deformation [105, 106].

To enable efficient solar energy harvesting and storage in flexible systems, AZIBs must simultaneously support low-rate charge acceptance, mechanical deformability, and structural compatibility with photovoltaic outputs. In this context, Zheng et al. [107] developed a cone-spinning strategy to fabricate carbon nanotube/manganese dioxide (CNT/MnO_2) composite yarn cathodes that are particularly well suited for integration with solar cells (Figs. 3(a)–3(c)). Unlike conventional Fermat-spun yarns, the cone-spun architecture forms a compact, gradient-packed mesoscale current-collecting network, facilitating rapid ion/electron transport and uniform current distribution under the

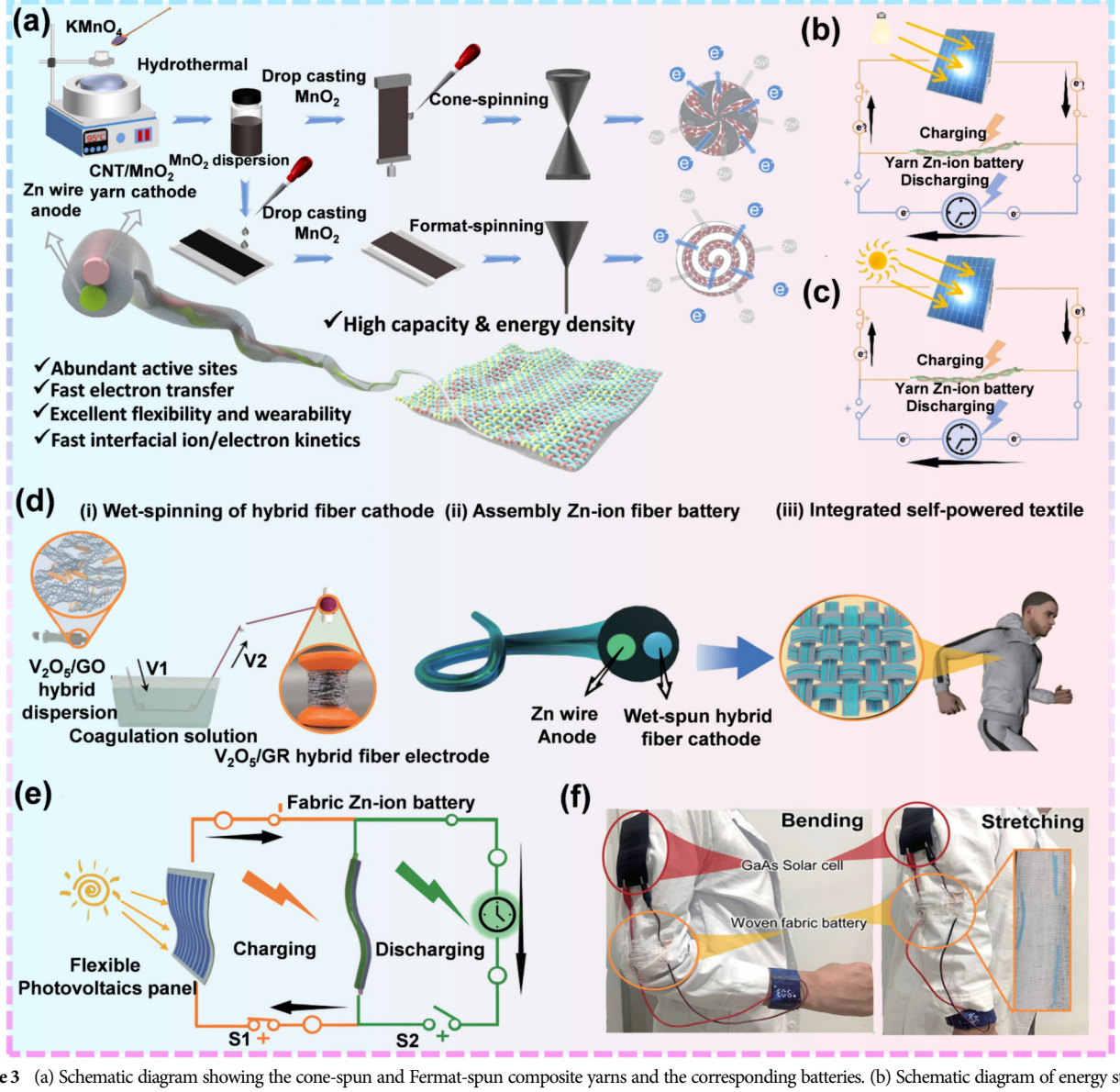

Figure 3 (a) Schematic diagram showing the cone-spun and Fermat-spun composite yarns and the corresponding batteries. (b) Schematic diagram of energy storage device. (c) Schematic diagram of the self-powered energy system. Reproduced with permission from Ref. [107], © Elsevier Ltd. 2025. (d) Schematic illustration of the wet-spinning, assembly and self-powered textile integration for the AZIBs. (e) Schematic illustration of an integrated self-powered textile. (f) Optical image demonstrating the wearable self-power integrated system. Reproduced with permission from Ref. [110], © Wiley-VCH GmbH 2022.

low and fluctuating charging currents characteristic of photovoltaic devices. Consequently, cone-spun CNT/MnO_2 yarn-based AZIBs exhibit exceptional photo-charge tolerance, delivering a high specific capacity of 490.4 mAh·g^{-1} and an energy density of 559.8 Wh·kg^{-1}, while retaining 86% of their capacity over 5000 cycles. More importantly, the dense CNT framework mitigates MnO_2 dissolution and polarization during intermittent solar charging, ensuring stable energy storage even under variable irradiance conditions. By directly coupling polycrystalline solar cells with the yarn-shaped AZIB string, a self-powered energy system was realized without relying on complex power-management circuitry. The photovoltaic units were electrically configured to provide a charging voltage window compatible with the operating range of the yarn batteries, enabling direct photo-charging. This solar–battery integration highlights a key advantage of yarn-shaped AZIBs, their capacity to function simultaneously as flexible energy-storage units and mesoscale current collectors capable of accommodating low-intensity, discontinuous solar inputs. Compared with previously reported photo-rechargeable fiber systems, such as fiber-shaped Zn–polyaniline (PANI) batteries and integrated energy-harvesting/storage fibers, this design demonstrates superior electrochemical robustness and mechanical stability under bending [108, 109]. Nevertheless, the direct-coupling strategy also indicates that the charging rate and state of charge remain susceptible to irradiance fluctuations and cell-to-cell variation, suggesting that future solar-integrated AZIB systems may benefit from adaptive voltage regulation or hybrid buffering architectures. Overall, this work underscores the potential of structurally engineered AZIB yarns as enabling components for flexible, wearable, and self-powered solar energy systems.

A key obstacle hindering the integration of AZIBs with photovoltaic modules is the challenge of fabricating mechanically robust, ion-transport-efficient fiber electrodes suitable for large-area energy textiles. To overcome this material–processing barrier, Shao et al. [110] used a wet-spinning approach compatible with large-area textile production and regulated the rheology of V_2O_5 nanowire dispersions via graphene oxide/reduced graphene oxide (GO/rGO)-induced viscoelastic and liquid-crystalline ordering. The resulting highly oriented V_2O_5/rGO fibers enabled fast Zn^{2+} transport and high electrochemical utilization, delivering 486.03 mAh·g^{-1} at 0.1 A·g^{-1} while retaining flexibility and durability under deformation—critical for stable operation under fluctuating photovoltaic charging currents. They further assembled a quasi-solid-state, half-meter fiber AZIB and integrated it with a GaAs solar cell, demonstrating practical solar–battery integration for wearable self-powered textiles. Compared with cone-spun yarns, wet-spun fiber architectures emphasize continuity in fiber length, controlled cross-sectional geometry, and stable fiber–electrolyte interfaces, enabling the scalable fabrication of energy textiles in which numerous AZIB fibers can be woven, knitted, or embroidered into fabrics that maintain uniform Zn^{2+} storage behavior across large areas [111–113]. Notably, when coupled with a GaAs photovoltaic module, these fiber-shaped AZIBs formed a wearable solar-charging system that achieved an overall solar-to-storage efficiency of 9.80% (Figs. 3(d)–3(f)). This high efficiency results from co-optimizing intrinsic AZIB properties such as internal resistance, ionic pathways, and the gel-electrolyte and encapsulation design with the output characteristics of the GaAs solar cell. This coordinated matching minimizes overpotential losses during intermittent illumination. Collectively, this work demonstrates how materials-level engineering of fibrous AZIBs can directly enhance the effectiveness of photovoltaic integration, offering a practical route toward deformable, textile-integrated, solar-rechargeable AZIB systems.

Despite these advances, solar–AZIB integration in fiber formats still faces unresolved bottlenecks including high internal resistance, encapsulation complexity, and durability under real-world wear conditions [104]. Maintaining stable charge acceptance during fluctuating irradiance requires co-optimization of fiber electrode conductivity, gel-electrolyte ionic pathways, and photovoltaic output matching. Recent progress in meter-long fiber AZIBs and energy textiles indicates that breathable encapsulation, self-healing electrolytes, and dendrite-suppressing anodes are critical for preserving electrochemical stability through stretching, laundering, and temperature cycling [114–117]. Future solar-rechargeable textiles will likely require coaxial photovoltaic (PV)–battery cable architectures, adaptive low-voltage power management, and scalable weaving or embroidery integration schemes to translate laboratory efficiencies into deployable wearable power platforms [118–121].

3.2 System integration of film batteries

Ultrathin film–type AZIBs have emerged as a practical platform for integrating solar harvesting and energy storage in flexible and wearable systems. Their cuttable, printable, and design-editable architectures enable precise control over thickness, geometry, and mechanical compliance—features essential for matching the form factors of planar photovoltaic modules and achieving deformation-compatible solar charging. Structurally, these film batteries are typically constructed either as in-plane printed paper cells, in which current collectors and electrodes are patterned on a flat substrate, or as laminated all-in-one films that combine current collectors, active layers, gel electrolytes, and encapsulation into a monolithic stack. Regardless of configuration, the primary engineering challenge is to co-optimize areal capacity, mechanical tolerance, and interfacial stability so that the AZIB can be seamlessly coupled with ultrathin solar cells, sensors, or electronic circuits without introducing mechanical or electrical discontinuities within the integrated system [122].

For instance, Fan et al. [123] proposed a printable paper-based AZIB as a system-level power module for sustainable paper electronics and solar-integrated wearables (Fig. 4(a)). By using hydrogel-reinforced cellulose paper (HCP) as both the separator and quasi-solid electrolyte, the Zn anode and MnO_2 cathode can be directly printed on opposite sides of the same substrate without risk of short-circuiting (Fig. 4(b)). This monolithic, cuttable battery-on-paper design is compatible with printed patterns and flexible circuits, provides stable output under repeated bending, and eliminates the need for bulky packaging, thereby simplifying integration into compact devices. When coupled with an amorphous silicon solar cell, the platform forms a deformable, self-powered paper system capable of real-time photocharging and continuous operation of small electronics, demonstrating a practical pathway toward integrated energy harvesting and storage on paper (Fig. 4(c)). Compared with more intricate PV–AZIB photo-rechargeable stacks, this planar Si–paper system places greater emphasis on structural compatibility, particularly the matching of thickness, flexibility, and bending radius between the paper battery and the ultrathin photovoltaic layer. Such "substrate-level" co-design ensures conformal contact, minimizes mechanical mismatch, and enables reliable solar-charging even during bending or folding. Although its conversion efficiency may be lower due to the simplicity of the lamination and wiring strategy,

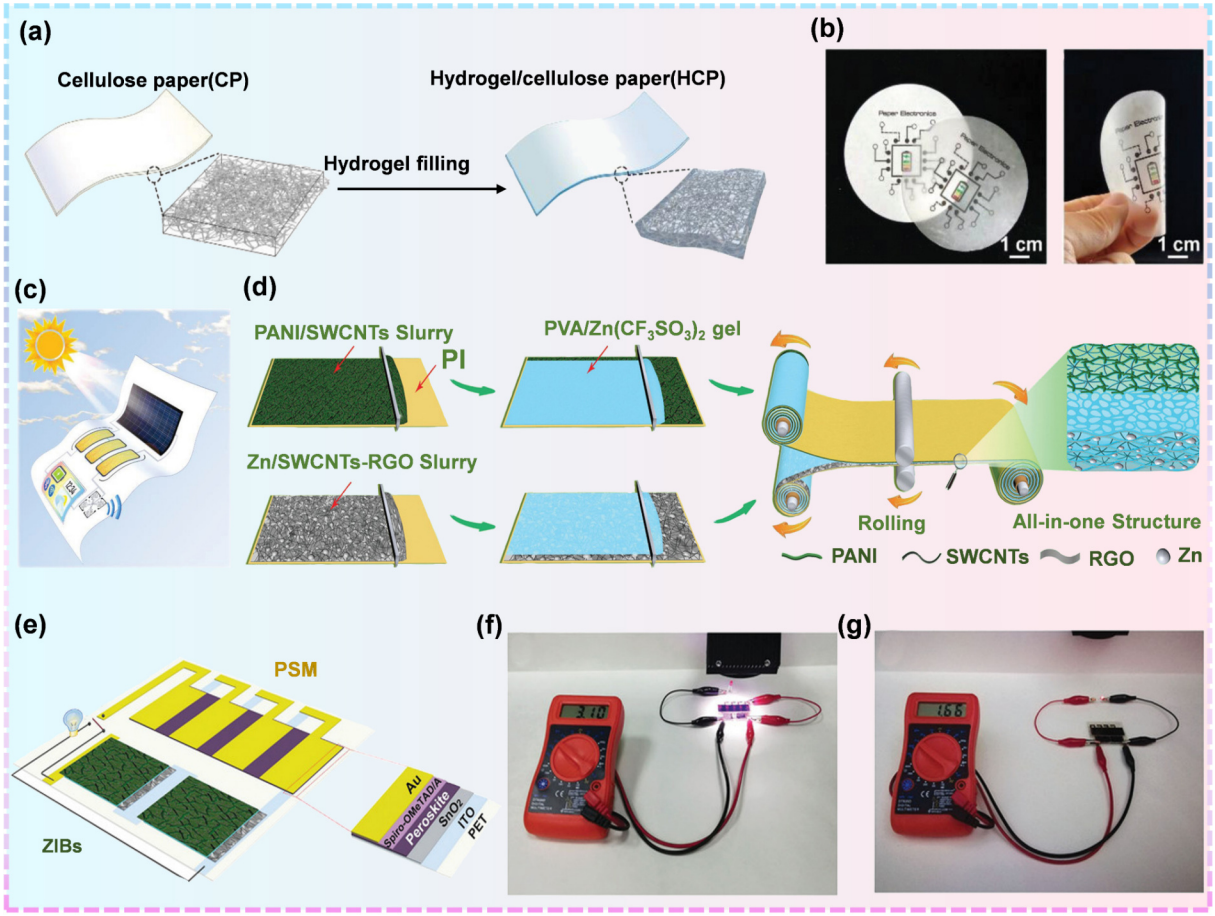

Figure 4 (a) Schematic of original commercial cellulose filter paper (CP) and HCP. (b) Optical image of HCP (top) and original CP (bottom) with printed circuit patterns and one piece of HCP under mechanical deformation. (c) Illustration of a self-powered system on paper. Reproduced with permission from Ref. [123], © Wiley-VCH GmbH 2022. (d) Schematic process, the design of ultrathin all-in-one AZIBs. (e) Diagram of the PSM-AZIBs. Optical images of the PSM-ZIBs under different states: (f) fully photo-charged; (g) delivering power to light an LED. Reproduced with permission from Ref. [122], © Wiley-VCH GmbH 2021.

the work demonstrates a scalable and eco-friendly route toward fully printed, solar-rechargeable energy modules for wearable and disposable electronics. Similarly, Niu et al. [122] proposed a scalable assembly strategy for ultrathin all-in-one AZIBs that directly addresses the structural and interfacial requirements of photovoltaic integration in wearable systems (Figs. 4(d) and 4(e)). By combining blade coating with rolling assembly, they constructed a monolithic configuration in which the cathode, gel electrolyte, and anode are unified into a continuous stack. This architecture enables uninterrupted ion and electron transport and maintains mechanical stability during bending or twisting—capabilities essential for matching the deformation profiles of ultrathin photovoltaic modules. The resulting film batteries are tailorable and shape-editable, allowing conformal integration with planar or flexible photovoltaic layers without disrupting charge flow or inducing mechanical mismatch. Compared with discrete layer-by-layer film cells, the monolithic design significantly reduces interfacial resistance and minimizes the risk of delamination during solar-charging cycles. However, achieving such structural continuity imposes strict requirements on slurry rheology, gel-electrolyte crosslinking behavior, and interfacial adhesion to prevent local strain accumulation and to maintain consistent ionic pathways under complex deformation [124–127]. Parallel advancements in reinforced cellulose and nanomicellar hydrogel electrolytes have demonstrated enhanced Zn^{2+} desolvation, suppressed dendrite growth, and retained mechanical integrity under deformation. These developments highlight the importance of mechanically robust, ion-regulating gels for stable photovoltaic-coupled AZIB operation [125]. Integration of these all-in-one AZIBs with a perovskite solar module (PSM) produced a compact photo charging system capable of efficient solar energy harvesting and storage (Figs. 4(f) and 4(g)). In this configuration, the PSM serves as a lightweight, high-voltage photovoltaic front end, while the ultrathin AZIB functions as a deformable, fast-response energy buffer. The strong structural compatibility between the PSM and the monolithic AZIB minimizes electrical and mechanical discontinuities, demonstrating a practical route for constructing photovoltaic-integrated ultrathin AZIB systems suitable for wearable and customizable electronics.

However, despite their strong potential for integration with photovoltaic modules, ultrathin AZIBs still face substantial challenges in scalable assembly, limiting the practical deployment of large-area solar-rechargeable systems. Current roll-to-roll and printing-compatible fabrication routes often suffer from thickness non-uniformity, interlayer defects, and inconsistent electrolyte uptake across wide-area films. Such manufacturing imperfections disrupt ionic and electronic continuity, generating local overpotentials and accelerating material degradation. In photovoltaic-coupled systems, where uniform charge acceptance is essential for stable photocharging, these inconsistencies may even lead to partial loss of self-powered functionality at the module scale [128–132]. Nevertheless, the combined advantages of cutability, printability, and modular compatibility highlight the

unique suitability of ultrathin AZIBs for photovoltaic integration in next-generation wearable electronics. Their ability to conform to ultrathin solar cells and maintain electrochemical stability under irradiation-induced temperature fluctuations or mechanical deformation underscores their promise as energy-buffer layers in integrated solar-charging platforms. Looking ahead, key device-level design principles from flexible AZIBs, including strain-tolerant current collectors, robust hydrogel electrolytes, and standardized solar-to-storage evaluation, can be applied to emerging photo-rechargeable architectures such as perovskite-coupled or polymer-photoelectrode AZIBs. Incorporating these strategies is expected to accelerate the transition of ultrathin zinc-ion film batteries from proof-of-concept systems to manufacturable photovoltaic-integrated technologies [133–135].

3.3 Solar-powered flexible zinc-ion energy storage

Integrating flexible aqueous zinc-ion batteries with photovoltaic devices requires resolving a fundamental electrochemical mismatch, as solar cells deliver fluctuating, low-current outputs whereas conventional MnO_2 cathodes exhibit sluggish charge-transfer kinetics and severe polarization that limit efficient energy capture [136]. This kind of system with separate photovoltaic and energy storage devices has a simple design but essentially comprises two independent devices with large volume and low integration, which easily causes external energy loss and high space occupancy. The second type is to integrate the photoelectrode and the energy storage battery into a single unit, called an integrated solar battery. At present, a significant challenge of the integrated solar battery is realizing the voltage and current matching between the photovoltaic conversion unit and the energy storage unit [137]. This mismatch becomes particularly acute at the high mass loadings (>20 mg·cm^{-2}) necessary for practical areal capacity, where limited electrical conductivity and slow Zn^{2+} diffusion further exacerbate charging inefficiency. To address this challenge, a defect-engineering strategy combining oxygen vacancies with expanded interlayer spacing has been developed to modulate the electronic structure and ion-transport pathways of MnO_2 nanosheets [138] (Figs. 5(a)–5(c)). The resulting cathode achieves accelerated electron transport and enhanced Zn^{2+} diffusion, thereby reducing polarization sufficiently to accept the approximately 1.1 V output from flexible perovskite solar cells with power conversion efficiencies exceeding 18%. At an ultrahigh mass loading of 25.5 mg·cm^{-2}, the quasi-solid-state battery delivers an areal capacity of 3.63 mAh·cm^{-2} while tolerating variable illumination, mechanical bending, impact, and temperatures spanning −20 to 80 °C, enabling smooth charging to approximately 5 V and sustained power delivery to wearable electronics over several hours.

Beyond cathode optimization, efficient solar–battery integration

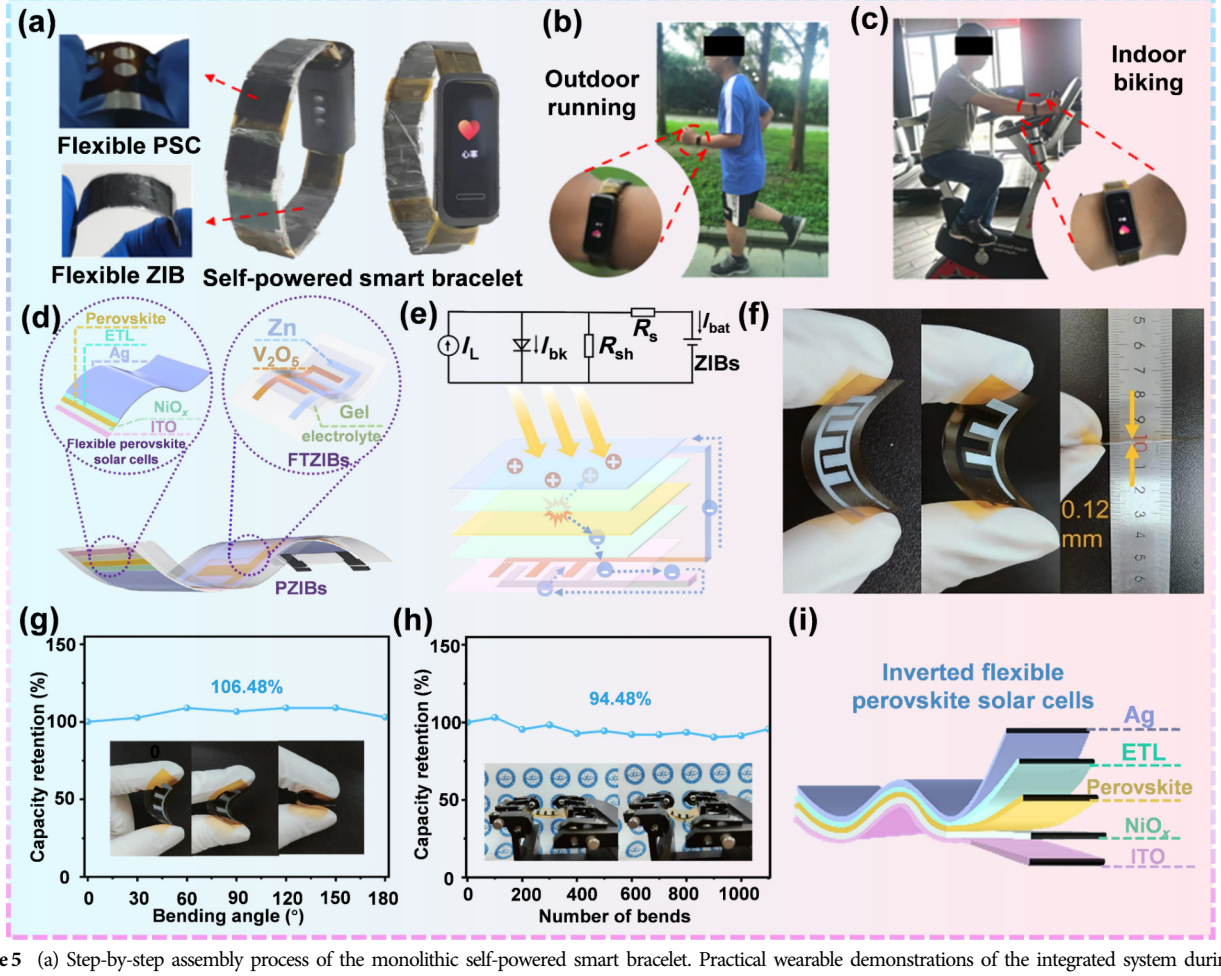

Figure 5 (a) Step-by-step assembly process of the monolithic self-powered smart bracelet. Practical wearable demonstrations of the integrated system during (b) outdoor running and (c) indoor cycling activities. Reproduced with permission from Ref. [138], © American Chemical Society 2021. (d) Schematic illustration of a photo-rechargeable zinc-ion battery (PZIB) architecture. (e) Charge transfer mechanism in portable PZIBs under solar illumination. (f) Photograph of the as-fabricated flexible thin-film zinc-ion battery (FTZIB). Mechanical flexibility evaluation: (g) single bending test and (h) cyclic bending durability assessment. (i) Device architecture of the inverted flexible perovskite solar cell. Reproduced with permission from Ref. [140], © Elsevier Ltd. 2025.

also demands a stabilized Zn interface capable of accommodating the rapid and fluctuating photocurrents characteristic of photovoltaic outputs. Key challenges such as low cell voltage, dendrite formation, passivation, and hydrogen evolution remain central obstacles to practical implementation [139]. In a complementary approach, an Ag–Cu current collector suppresses galvanic corrosion of the Zn thin film, while a zwitterionic organohydrogel regulates Zn nucleation to prevent dendrite formation and preserves ion-transport pathways under mechanical deformation [140]. These interfacial reinforcements collectively reduce polarization, enabling the thin-film battery to accept transient charging pulses without capacity fade (Figs. 5(d)–5(f)). Architecturally, fabricating the perovskite solar cell and the battery on opposite sides of a single polyimide substrate eliminates external wiring and lowers interfacial impedance at the harvesting–storage junction. The resulting monolithic device achieves an overall solar-to-storage conversion efficiency of 18.44%, the highest reported value among portable photo-rechargeable wearable AZIB systems (Figs. 5(g)–5(i)).

Integrating solar cells and AZIBs into a single device for energy conversion and storage offers several benefits, including space savings, reduced material use, increased portability, and enhanced flexibility. These batteries are efficient in energy storage and photo-rechargeable, making them promising candidates for sustainable energy use [141]. The growing demand for renewable energy has heightened the need for efficient energy storage solutions. As the reliance on renewable energy sources increases, the integration of robust energy storage systems is essential to stabilize the grid and compensate for periods of low wind or low sun.

Nevertheless, commercialization efforts are bottlenecked by active material dissolution, a lack of realistic performance demonstrations, and the need for manufacturing validation and cost analysis at the pilot scale [142]. Despite considerable progress in enhancing performance at room and low temperatures for large-scale applications, maintaining functionality at high temperatures remains a major challenge, restricting the use of safe, biocompatible, and body-adaptive AZIBs in small-scale wearable and implantable technologies. Together, these advances demonstrate that mechanism-guided defect modulation at the cathode, coupled with interface stabilization at the anode and monolithic architectural design, can reconcile the kinetic demands of solar charging with the capacity and durability requirements of flexible energy storage, providing foundational design principles for solar-rechargeable wearable AZIB systems. Future progress will require not only improvements in electrode kinetics and interfacial stability but also the development of standardized testing protocols that bridge laboratory-scale demonstrations with real-world performance metrics [143, 144].

3.4 Wearable energy applications integrated with AZIBs

Integrating mechanical energy harvesters with AZIBs has become an attractive strategy for constructing autonomous self-powered systems, as it enables the direct conversion and storage of biomechanical energy generated during human motion. For AZIB-based systems, the key challenge lies in ensuring that the battery maintains mechanical flexibility, stable charge acceptance, and long-term durability under the irregular, low-frequency mechanical inputs typical of wearable environments. As wearable electronics increasingly demand sustainable and maintenance-free power sources, coupling AZIBs with mechanical energy harvesters offers a promising pathway toward continuous, motion-driven energy replenishment.

The mechanical-electrochemical mismatch inherent to wearable AZIB operation underscores the need to harvest motion energy as a compensatory charging pathway. Zhi et al. [145] demonstrated an effective mechanical-energy-to-zinc-storage system by directly integrating triboelectric nanogenerators (TENGs) with flexible AZIBs on a 3D spacer textile (Fig. 6(a)). The textile framework supports scalable, multipixel AZIB arrays and provides mechanical compliance suited for wearable applications. Within this architecture, the upper and lower conductive fabric layers simultaneously function as triboelectric electrodes for mechanical energy harvesting and as current collectors for multiple AZIB cells, enabling straightforward series or parallel integration to tune charging voltage and current. During periodic mechanical stimuli, such as hand pressing, the TENG converts contact–separation motions into electrical pulses that are rectified and used to recharge the AZIBs, increasing their voltage from 0.93 to 1.28 V within 30 minutes and delivering a discharge capacity of 10.9 μAh at 4 μA (Fig. 6(b)). The 3D spacer structure, consisting of two conductive layers separated by an elastic intermediate layer, ensures both efficient triboelectric energy generation and stable electrochemical performance under bending and repeated compression. This hybrid TENG–AZIB textile system can reliably power small electronics such as digital watches, demonstrating its potential as a flexible, scalable, and fully integrated platform for mechanical-energy-driven zinc-ion storage. These results underscore the feasibility of AZIB-based self-powered architectures for future wearable, energy-autonomous electronic systems.

Achieving sustainable power supply for wearable electronics remains a critical challenge, as conventional systems depend on external charging sources that fundamentally constrain device autonomy and practicality. Integrating mechanical energy harvesting with AZIBs offers a compelling strategy to address this bottleneck by converting ambient biomechanical motion into storable electrical energy. Ge et al. developed a polyvinyl alcohol/polyacrylamide/zinc sulfate (PPZ) hydrogel via one-step ultraviolet (UV)-initiated polymerization, where the hydrogen-bonded polyvinyl alcohol (PVA)- polyacrylamide (PAM) dual-network provides exceptional stretchability (915% strain) while Zn^{2+} incorporation simultaneously enhances ionic conductivity for both triboelectric generation and electrochemical storage [146] (Figs. 6(c)–6(e)). In the single-electrode TENG configuration, the PPZ hydrogel functions as both triboelectric layer and current collector, converting mechanical energy from contact-separation cycles into electrical output through coupled triboelectrification and electrostatic induction at the silicone rubber interface. Under optimized conditions, the PPZ-TENG achieves an open-circuit voltage of 176 V, short-circuit current of 3.56 μA, and maximum power density of 328 $mW \cdot m^{-2}$, maintaining stable output over 12,000 cycles. Critically, the same PPZ hydrogel serves as the electrolyte in a flexible AZIB with MnO_2 cathode and Zn anode, exhibiting ~1.15 V open-circuit voltage and stable performance under bending deformation. By rectifying the TENG's alternating current output and coupling with the AZIB, the integrated system charges the battery from 0.9 to 1.23 V within 956 s at 3 Hz operation, thereby establishing a closed-loop energy harvesting-storage cycle that enables truly self-sustainable wearable power systems without external energy input (Figs. 6(f)–6(h)).

In summary, wearable AZIBs integrated system with energy harvesting capability enables simultaneous capture of environmental energy and electrochemical storage, which not only overcomes the reliance of traditional AZIBs on external power

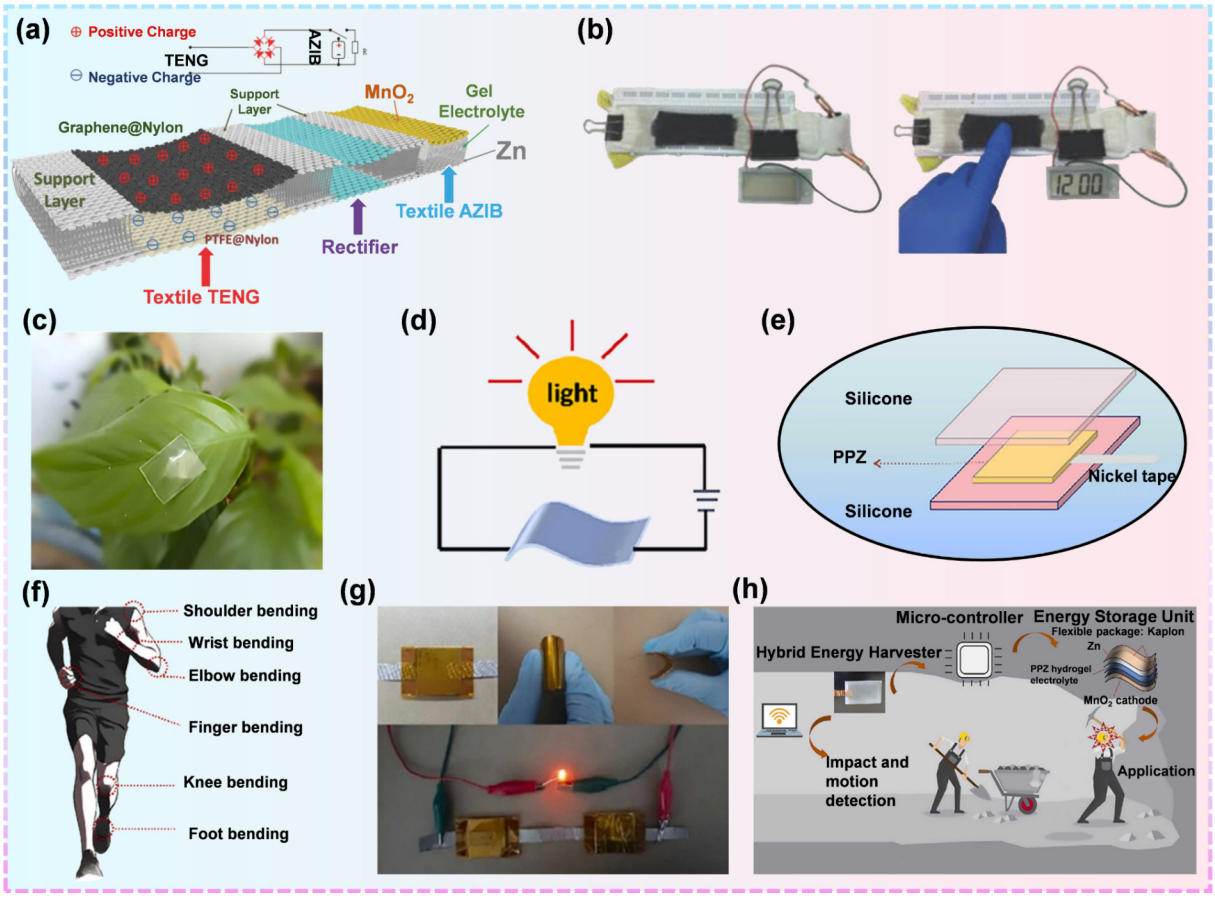

Figure 6 (a) The schematic diagram of the three-dimensional (3D) spacer fabric-based energy harvesting and storage device. (b) Demonstration showing an electronic watch powered by the flexible AZIBs charged by the TENG through hand press. Reproduced with permission from Ref. [145], © Wiley-VCH GmbH 2018. (c) Photograph of the transparent PP hydrogel conformally attached to a leaf surface. (d) Equivalent circuit diagram of the PPZ hydrogel-based energy harvesting module. (e) Exploded-view schematic of the PPZ-TENG device architecture. (f) Illustration of wearable sensor placement on the human body for biomechanical motion detection using self-powered PPZ-TENG sensors. (g) Photographs of the flexible AZIBs under flat and bent states, with light emitting diode (LED) illumination powered by two serially connected batteries. (h) Conceptual demonstration of the integrated PPZ-TENG and AZIB system for autonomous wearable energy harvesting and storage applications. Reproduced with permission from Ref. [146], © Elsevier Ltd. 2024.

sources but also fully leverages the inherent advantages of AZIBs in terms of safety, cost-effectiveness, and environmental friendliness. This lays a critical technological foundation for constructing highly integrated and reliable self-powered wearable AZIB system.

4 Energy sensing

Through synergistic optimization of energy management and information perception, the integration of wearable AZIBs with sensing modules constructs a closed-loop intelligent system capable of self-sensing and self-powering. This system not only enhances monitoring accuracy but also achieves self-calibration functionality. It provides a stable, efficient, and self-consistent solution for real-time, continuous, and long-term vital sign monitoring or adaptive human-machine interfaces.

4.1 Mechanically responsive self-powered zinc-ion systems

Bridging energy storage and sensing, recent AZIB platforms are being designed so that mechanical deformation directly regulates Zn-ion transport and deposition, enabling battery-as-sensor integration. Zhang et al. reported a PAM/polyvinylidene fluoride@UiO-66 (PAM/PVDF@UiO-66, PPM) composite membrane that couples a piezoelectric-induced piezo-ionic effect with aqueous Zn-ion electrochemistry, allowing one material layer to function as both a flexible sensor and an AZIB electrolyte/separator [147] (Figs. 7(a)–7(c)). Under pressure, polarization of the PVDF-based fiber network generates an internal electric field that accelerates ion migration and redistributes local Zn^{2+} flux, improving signal transduction and promoting uniform Zn nucleation to suppress dendrites. As a result, the membrane delivers ultrafast sensing with electrical outputs up to 23.64 μA, while also supporting dendrite-free symmetric cycling for 2000 h and a stable battery capacity of 150 $mAh \cdot g^{-1}$. Although the harvested power is typically modest and is more suitable for self-powered sensing than rapid energy replenishment [148–150], the integrated AZIB system enables light-, pressure-, and motion-responsive monitoring, supporting wearable functions such as facial-expression recognition and intelligent motion guidance with accuracies above 94%.

Beyond piezoelectric approaches, designing wearable AZIBs to function as pressure sensors represents another important strategy for creating compact and self-powered sensing systems. Although these devices focus on signal transduction, their working principles remain closely related to those of mechanically driven wearable AZIBs, as both depend on the interaction between mechanical stimuli and zinc-ion electrochemistry [151, 152]. The sensing mechanism arises from pressure-induced changes in

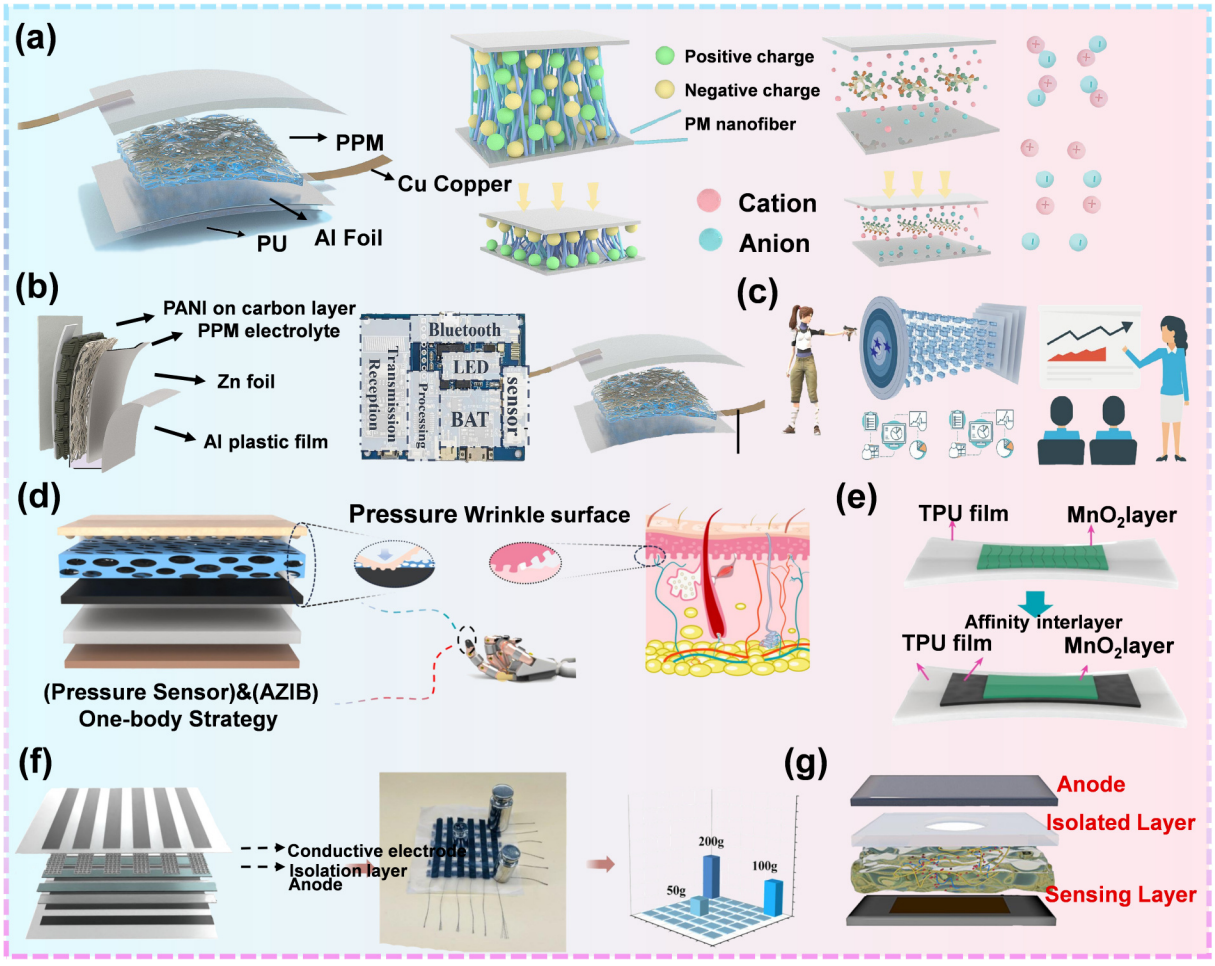

Figure 7 (a) Working principle and electrical output performance of piezoelectric ion sensor based on PPM composite agglutination fiber with the structure of PPM piezoelectric ion sensor, the working principle of piezoelectric sensor and PPM piezoelectric ion sensor. (b) Power supply unit of the flexible sensing system. (c) Intelligent training system, applications of PPM sensors. Reproduced with permission from Ref. [147], © Elsevier Ltd. 2025. (d) Overall design strategy diagram of the AZIB-flexible pressure sensor. and schematic diagram of the multilayered hierarchical structure of human skin. (e) Schematic illustration of the structure of the micro electrodes. (f) 6 × 6 matrix of pressure sensors (schematic and physical) and pressure mapping of objects. Reproduced with permission from Ref. [153], © Elsevier Ltd. 2024. (g) Overall design strategy diagram of the gelatin battery pressure sensor. Reproduced with permission from Ref. [156], © Elsevier Ltd. 2024.

internal resistance or electrode potential, where mechanical deformation modifies ion transport and the electrical response of the cathode, directly converting mechanical stimuli into measurable electrical signals. The pressure-modulated contact area strategy exemplifies this approach by converting mechanical deformation into electrical signals through controlled changes at the electrode–electrolyte interface. Guo and co-workers constructed a conductive layer decorated with PMMA microspheres, a porous spacer, and a flexible zinc anode integrated with a PVA and GO gel electrolyte [153] (Fig. 7(d)). The engineered concave and convex interface prevents hydrogel adhesion and converts applied pressure into resistance changes, enabling the AZIB to function in a self-powered sensing mode with an open-circuit voltage of 1.46 V and an energy density of 392 μWh·cm^{-2}. Compression increases the electrode–gel contact area, which facilitates ion transport and charge transfer and thereby lowers internal resistance and polarization. Consequently, under a fixed load, the output voltage or current increases with applied pressure, enabling self-powered sensing. The device conforms to soft surfaces and detects balloon expansion, finger bending between 30° and 90°, and wrist pulse features, while two series-connected units can power two LEDs while encoding pressure signals (Figs. 7(e) and 7(f)). Since porous spacers add inactive volume, recent studies focus on refining spacer geometry to improve sensitivity while maintaining continuous ion pathways [154, 155]. To further simplify the structure, a battery-type pressure sensor in which a gelatin–chitosan (GEL–CTS) composite hydrogel serves simultaneously as the electrolyte and pressure-sensing layer, while a thin polydimethylsiloxane (PDMS) isolation layer keeps the device in an open-circuit, zero-signal standby state until loading occurs [156] (Fig. 7(g)). Upon compression, the PDMS barrier is progressively weakened, enabling Zn^{2+} transport through the GEL–CTS membrane and generating a stable direct-current (DC) voltage signal that directly tracks pressure, which allows reliable static pressure monitoring for >10,000 s. This integrated design delivers fast response/recovery, high sensitivity and a wide pressure window, and it also shows broad electrode/material compatibility, supporting practical integration into flexible AZIB systems without complex external circuitry. As a proof of application, the concept was scaled to a 7×5 pressure-mapping array with biodegradable encapsulation, highlighting its potential for self-powered electronic skin and biomedical pressure monitoring where long-term static signals and low standby power are essential.

These examples, together with emerging hydrogel-based TENG

and zinc-ion hybrids, suggest that future self-powered AZIBs will increasingly adopt monolithic or modular architectures in which shared gel or polymer frameworks support both mechanical energy harvesting and zinc-ion storage. However, this integration introduces inherent trade-offs. Improving flexibility often lowers energy density and increases the need for strong interfacial engineering to maintain stability during repeated deformation. A major technical challenge is the impedance mismatch between TENG or piezoelectric harvesters and AZIBs, as the harvesters usually output intermittent signals with high impedance while AZIBs require continuous charging at low impedance. Solving this mismatch often requires rectifiers or charge management circuits, which introduces additional losses, added bulk, and extra points of failure [157, 158]. Mechanical compatibility also remains difficult to achieve, since soft and breathable textiles support wearability but conflict with the protection of zinc anodes and with stable electrolyte retention, and reliable encapsulation that is both leak-proof and ion-conductive is still lacking [159, 160]. Furthermore, repeated deformation may lead to hydrogel fatigue and interfacial failure, highlighting the need for tougher and self-healing polymer networks as well as monolithic architectures that reduce interfacial impedance [161, 162]. Progress therefore depends on the establishment of standardized metrics for conversion efficiency, charge delivery per cycle, and system-level reliability, while multiphysics modeling can further guide materials selection and device design [163, 164]. Fully stretchable textile systems remain promising, although their continued development will rely on improved energy management strategies and on more resilient materials with high electrochemical stability.

4.2 Self-powered sensor designs and applications of AZIBs

A major challenge for AZIB based pressure sensors is the need to maintain stable signal transduction while preserving device compactness and energy storage capability. Monolithic architectures that combine pressure sensing and zinc ion storage within a single device have therefore become an effective strategy. Gao et al. [165] developed a monolithic AZIB pressure sensor in which the battery itself operates as the sensing unit. A PVA nanofiber isolation layer was introduced into a sandwich configuration and paired with a PVDF-hexafluoropropylene-graphene oxide solid electrolyte. This arrangement enables pressure detection through internal resistance modulation (Figs. 8(a)–8(c)). The device shows response and recovery times of 76 and 88 ms, an ultrawide detection range from 2 Pa to 3368 kPa, and stable performance for more than 100,000 cycles. It also supports dual voltage and current operation with very low standby loss. The open circuit voltage is about 1 mV. The sensor detects pressures as low as 2 Pa, remains stable for 24 h, retains signals for thirty days, and fully restores its open circuit potential after repeated charge and discharge. The integrated device can monitor pulse waves including P, T, and D waves, track limb motion, and light LEDs when two units are connected in series. The system also exhibits material universality when used with VO_2, manganese hexacyanoferrate (MnHCF), or MoS_2 cathodes, which allows tuning of output and sensing performance. Interface engineering represents another effective method to enhance pressure sensitivity in AZIB based sensors. This approach relies on micro-structured electrode surfaces that enlarge the pressure responsive contact area. It helps overcome interfacial limitations inherent to these systems [166, 167]. It differs from strategies that rely only on bulk resistance modulation. Micro-structured interfaces enable higher sensitivity by optimizing the electric double layer and charge transfer behavior at the same time. Using this concept, Zhang et al. [168] prepared a thorn like polyaniline composite that serves as the active electrode in a solid state AZIB and also as the sensing layer in a flexible pressure sensor. A layer-by-layer assembly method was used (Figs. 8(d)–8(f)). Upon pressing, the thorn-like microstructure is compressed, increasing the real contact area and facilitating interfacial ion adsorption and charge transfer. This reduces polarization and converts pressure into a reproducible change in the AZIB output or resistance, enabling high sensitivity. The system delivered a specific capacity of 405.07 mAh·g^{-1}, a sensitivity of 5.64 × 10^5 kPa^{-1}, rapid response and recovery times of 60 and 80 ms, a detection ranges from 50 Pa

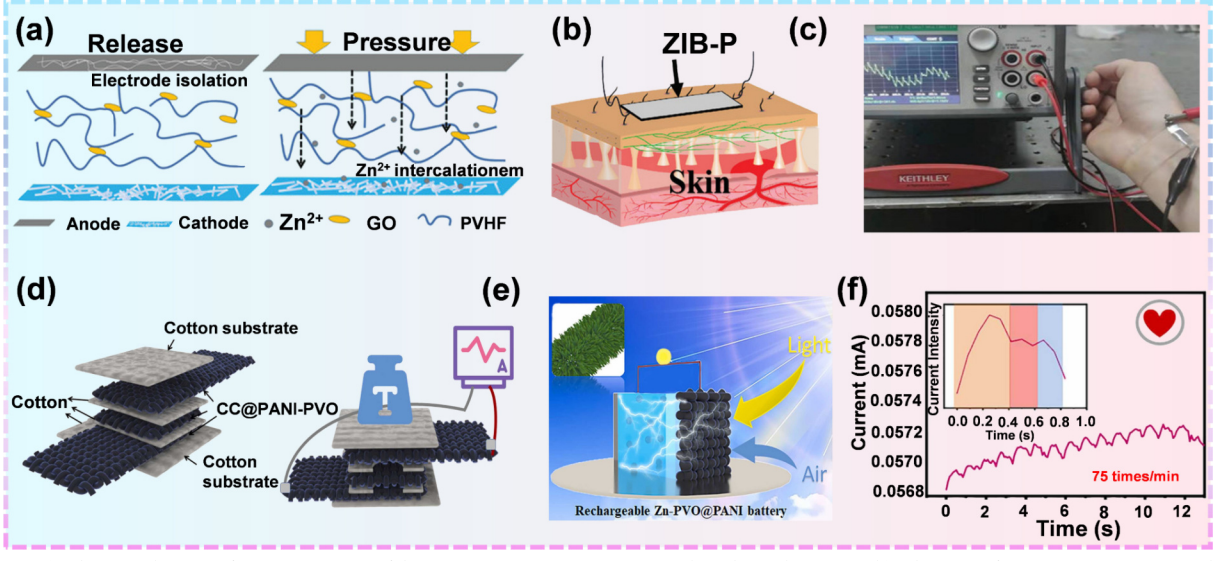

Figure 8 (a) Schematic diagram of response process of the AZIBs-pressure sensor to external mechanical pressure. (b) Schematic of AZIBs-pressure sensor to human pulse. (c) Photo of the AZIBs-pressure sensor attached to the human wrist for real-time monitoring of the pulse signal. Reproduced with permission from Ref. [165], © Wiley-VCH GmbH 2022. (d) A schematic illustration of an all-fabric tactile sensor and schematic diagram of the measurement principle of the sensor. (e) Air and light dual-assisted self-powered Zn–PANI battery. (f) The ultra-sensitive, self-powered sensor integrated system is used for pulse monitoring, blow detection, and even real-time response to rice-grain-sized polyurethane particle. Reproduced with permission from Ref. [168], © Elsevier Ltd. 2022.

to 70 kPa, and stable operation over 8000 cycles. These developments illustrate that AZIB based sensors can achieve compact design, self-powered operation, and high sensitivity through the combined use of structural optimization and interface engineering. They provide a promising platform for wearable electronic skin and autonomous intelligent systems integrated with AZIBs.

In summary, these battery–sensor hybrids show that aqueous zinc-ion batteries can achieve simultaneous energy storage and pressure sensing through interface and structural engineering. Monolithic designs and micro-structured electrodes demonstrate that regulating the electrode–electrolyte contact state is key to maintaining signal stability and high sensitivity. Although current devices still depend on stored electrochemical energy, their sensing mechanisms provide a foundation for developing fully self-powered systems. Transitioning from passive resistance modulation to active mechanical-energy harvesting will require interfaces that couple mechanical stress with electrochemical potential changes [169–171]. Despite fabrication challenges, one-body architectures offer a practical way to minimize interfacial resistance and material mismatch. Continued advances in interfacial engineering are expected to further enhance sensitivity and support the development of integrated AZIB-based platforms for electronic-skin, smart-home devices, and autonomous monitoring.

4.3 Hydrogel sensors and integrated wearable devices

Hydrogel-based sensors play an important role in wearable AZIB systems because their high ionic conductivity, mechanical compliance, and intrinsic mechanoelectrical responsiveness allow hydrogels to act as both electrolytes and active sensing elements. Their ability to convert deformation, pressure, or strain into ionic or electrical signals supports the creation of fully integrated and self-powered sensing modules. Effective design relies on the separation of ionic and electronic transport. It also requires stable mechano-electrochemical coupling and a balance between ionic conductivity and mechanical durability to maintain long-term sensing performance. Recent studies increasingly emphasize these requirements when examining relationships between hydrogel structure and properties, the stability of zinc and hydrogel interfaces, and the practical needs of hydrogel-based sensing components in flexible AZIBs [172].

Hydrogel microstructuring provides an effective route to enhance pressure sensitivity in AZIB-based wearable sensors. Zhou et al. [173] designed a locust bean gum/polyvinyl alcohol/carbon nanotube hydrogel with double-rough interfaces, achieving piezoresistive sensitivities of 20.5 kPa^{-1} (0–1 kPa) and broad-range detection (0.1–100 kPa). When monolithically integrated with flexible AZIBs, it enables stable self-powered motion sensing over 1000 cycles (Figs. 9(a)–9(c)). The amplified sensitivity originates from the roughened contact surfaces, while the CNT network maintains robust ionic–electronic transmission during deformation. However, enhancing surface responsiveness alone cannot ensure stable ion transport under large or repeated deformations, which highlights the need for deformation-tolerant

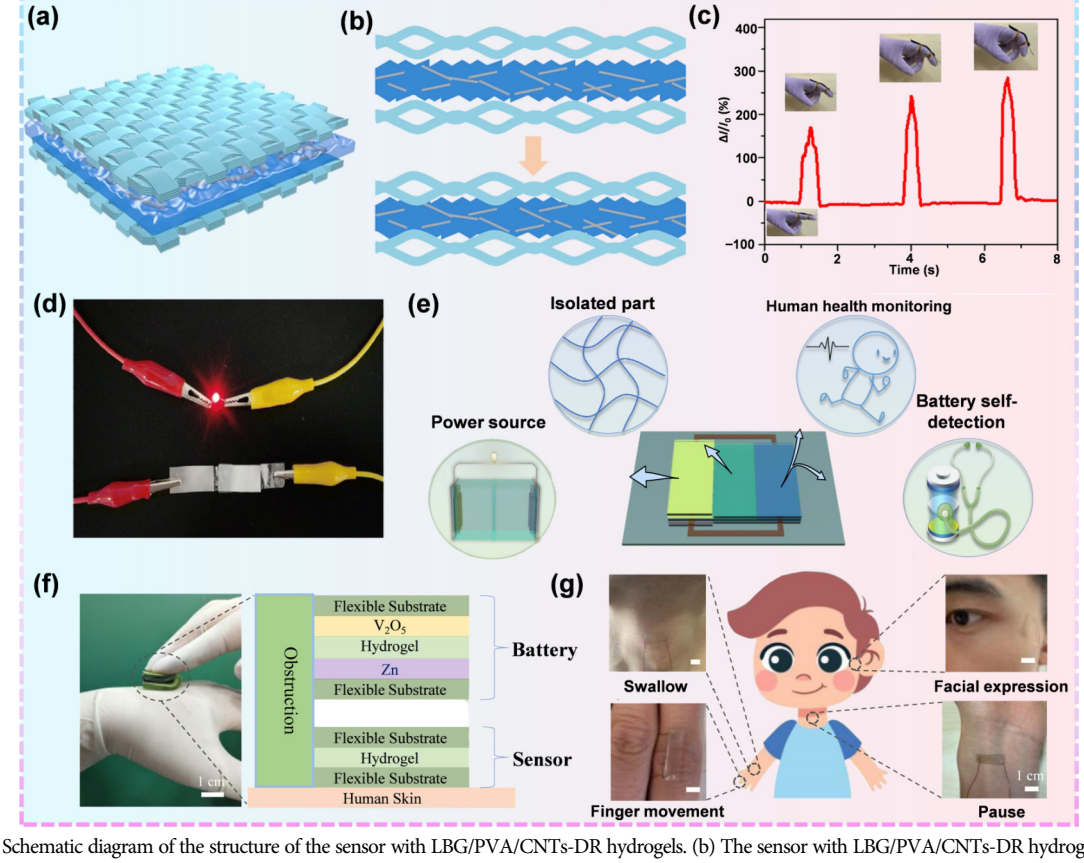

Figure 9 (a) Schematic diagram of the structure of the sensor with LBG/PVA/CNTs-DR hydrogels. (b) The sensor with LBG/PVA/CNTs-DR hydrogels' mechanism analysis of the pressing process. (c) The signal responses arise from finger bending. Reproduced with permission from Ref. [173], © Spring Nature 2022. (d) A 1.8 V LED can be efficiently powered by two AZIBs in series connection. Reproduced with permission from Ref. [174], © The Royal Society of Chemistry 2023. (e) Integrated strategy of the multifunctional device and schematic of the structural design. (f) Schematic of folding the wearable device in half on the skin for actual use. (g) Schematic and digital photos of wearable sensors attached to different parts of the human body for sensing various signals. Reproduced with permission from Ref. [178], © Elsevier Ltd. 2025.

hydrogel networks. Addressing this, Han et al. [174] developed a polyacrylamide/carboxymethyl cellulose/tannic acid (PAAM/CMC/TA) ionic hydrogel containing $ZnSO_4$ and $MnSO_4$ that combines high stretchability (622%), self-healing capability, and high ionic conductivity (0.76 ± 0.04 $S \cdot m^{-1}$). Serving as both the strain-sensing medium and the electrolyte in Zn // MnO_2 batteries, it maintains capacities up to 223.0 $mAh \cdot g^{-1}$ and stable output under deformation (Fig. 9(d)). Under strain, deformation alters the hydrogel geometry and ion-conduction pathways, producing a measurable change in ionic resistance and thus in the battery output under a given load. Meanwhile, dynamic crosslinking and self-healing restore the network after stretching, stabilizing ion transport and enabling repeatable strain sensing during large or cyclic deformations. Its mechanical resilience originates from dynamic crosslinking that preserves ion-transport pathways under strain. Such network engineering is key to ensuring stable sensing–energy-storage decoupling in hydrogel-based AZIBs [175, 176].

Further refinements in hydrogel composition such as PAAM, CMC and LiCl systems [177] introduce antifreezing capability down to −48.27 °C and ionic conductivity of 0.56 $S \cdot m^{-1}$. These properties allow a single flexible AZIB to support both energy storage and strain sensing under continuous mechanical input. The main mechanism involves regulating free water through a water and ethylene glycol mixed solvent. This approach suppresses ice formation and expands the operating temperature window. LiCl also supplies additional ionic carriers. This temperature adaptive strategy illustrates how hydrogel electrolytes maintain self-powered sensing and energy storage performance in harsh environments. Achieving multiple functions often introduces trade-offs. For example, extreme stretchability and self-healing may slow the response speed or lower the energy density. $ZnCl_2$-loaded poly(acrylic acid)-based composite hydrogels (Zn-PAA-C) offer a practical route to wearable, self-powered AZIB systems that combine strain sensing, Zn-ion transport, and battery self-diagnosis in one material platform. By engineering ionic coordination within a poly (acrylic acid) N-hydroxysuccinimide ester (PAA-NHS)/gelatin network and using an ethylene glycol/water solvent, the hydrogel maintains high ionic mobility and mechanical compliance while remaining freeze-resistant down to −80 °C [178]. As a strain sensor, it provides a broad working window (0–180% strain) and a fast response (~57 ms), enabling real-time motion/strain monitoring (Figs. 9(e)–9(g)). When used as a flexible AZIB electrolyte, the same ion-conductive matrix supports long-term cycling and, importantly, enables *in situ* safety monitoring, allowing real-time detection of battery swelling and Zn dendrite formation.

A comparison of these strategies reveals three connected design principles for hydrogel based self-powered sensing and energy storage systems. At the material level, dynamic crosslinked networks maintain ion transport pathways during deformation and ensure mechanical robustness and electrochemical continuity. At the structural level, anisotropic or gradient architectures help redistribute stress and reduce the trade-off between ionic conductivity and mechanical strength. At the functional level, multimodal sensing of strain, temperature and battery health combined with multiple forms of energy replenishment including electrochemical and chemical self-powered supports closed loop and autonomous operation. Looking ahead, research should focus on improving self-powered efficiency, developing degradable and biocompatible hydrogels for implantable AZIB systems, and using machine learning guided materials design to accelerate optimization across multiple objectives [179, 180]. Overall, strategic hydrogel innovation supports self-powered sensing and energy storage within AZIBs. It also provides environmental resilience and self-diagnostic capability, positioning hydrogels as key components for next generation wearable biomedical devices.

4.4 Multifunctional sensing-integrated AZIBs

Integrating sensing functionality directly into AZIBs represents an emerging strategy that unifies energy storage and signal transduction within a single electrochemical platform, eliminating conventional multi-component integration complexity while enabling self-powered operation. Hybrid microgrids coupling energy harvesting with AZIB storage exemplify this concept for autonomous biochemical sensing, as demonstrated by Wang et al. who developed a fingertip-wearable microgrid integrating enzymatic biofuel cells with AgCl–Zn batteries to harvest and store bioenergy from sweat, enabling autonomous multi-metabolite sensing of glucose, vitamin C, lactate, and levodopa in conjunction with low-power electronics for signal acquisition and wireless transmission [181] (Figs. 10(a) and 10(b)). Beyond biochemical detection, translating electrode microstructure into ionic signals offers a direct route for AZIB-based tactile sensing. The self-powered MXene–Zn^{2+} sensor generates pressure-responsive signals through Zn^{2+} migration without external power supply, inspired by biological skin-like ion-mediated sensing [182]. In this holey-MXene monolithic architecture, in-plane mesopores reduce ion-transport tortuosity; under applied pressure, expanded electrolyte–electrode contact shifts the low-frequency

Nyquist arc leftward and sharply lowers interfacial impedance, enabling approximately 49 ms response time and extended linear detection range when microstructured gel interlayers delay interfacial saturation (Figs. 10(c) and 10(d)). Compared with conventional capacitive sensors, Zn^{2+}-based devices provide enhanced resistance to environmental noise, humidity, and electromagnetic interference [183], while all-in-one designs convert pressure-modulated internal resistance into electrical outputs, greatly simplifying device architecture [184]. To address the inherent conflict between electrochemical stability and mechanical compliance, hydrogel-mediated designs assign both functions to a single ionic matrix. The PSC hydrogel serves simultaneously as the electrolyte for a Zn // V_2O_5 microbattery and as the strain-sensing layer, eliminating interfaces between energy and sensing modules [152] (Figs. 10(e) and 10(f)). The reinforced polymer network retains 42 $mS \cdot cm^{-1}$ conductivity at −20 °C, regulates Zn^{2+} solvation to homogenize deposition, and accommodates cathode lattice breathing across −20 to 80 °C. *Operando* XRD confirms that cathode phase evolution correlates directly with Zn plating/stripping-induced strain, establishing intrinsic coupling between electrochemical state and mechanical output. Extending operational robustness to extreme environments, deep eutectic/ionic-liquid composite gels reconstruct the hydrogen-bond network to create water-poor coordination environments, suppressing free-water activity and homogenizing Zn deposition to yield 1003 h Zn // Zn cycling at 2 $mA \cdot cm^{-2}$ and stable Zn // VO_2 operation from −20 to 80 °C [185] (Fig. 10(g)). The same molecular design confers 2500% stretchability, continuous ion-transport pathways under load, and strong adhesion to electrodes and biological tissue, allowing geometry-induced resistance changes to be transduced during bending, stretching, or joint motion (Fig. 10(h)). Collectively, these advances establish that AZIB-based sensors require high active-site

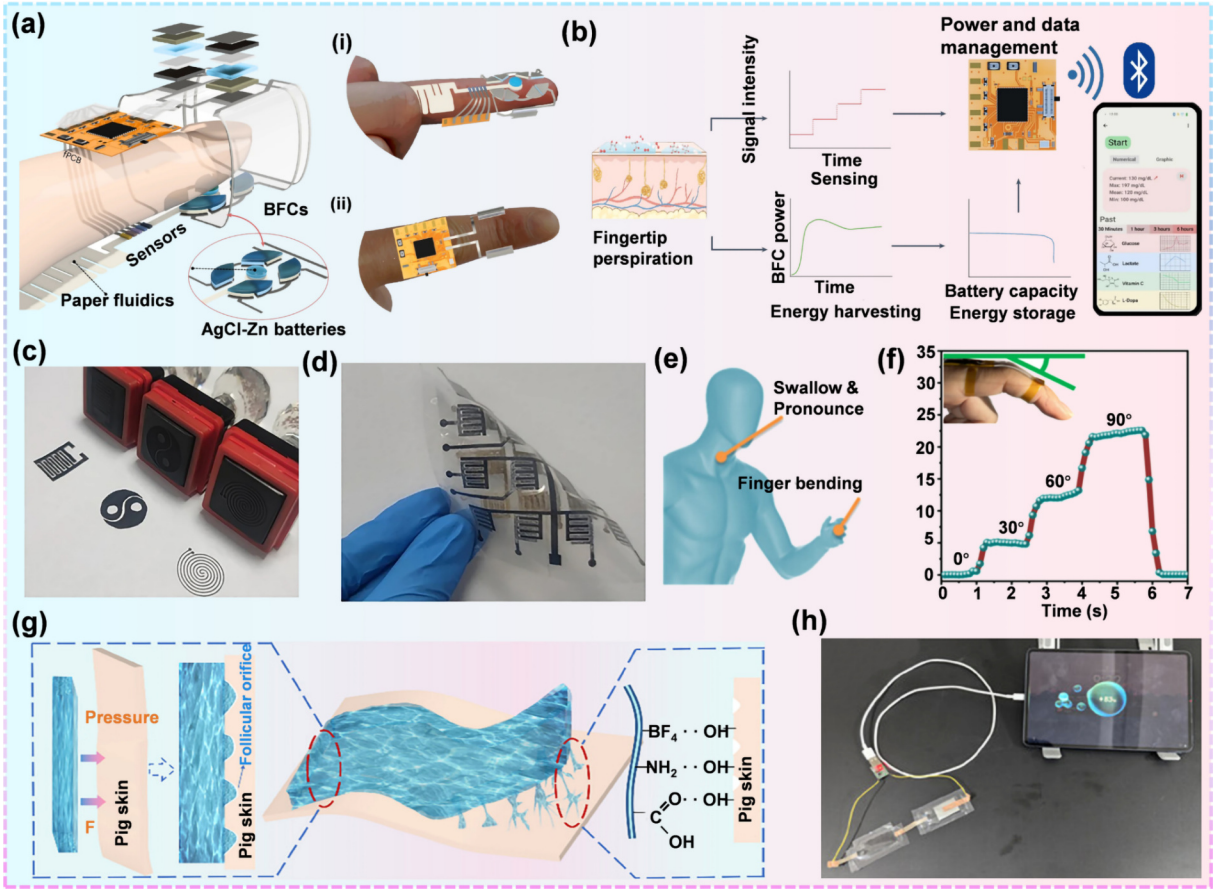

Figure 10 (a) Schematic of fingertip microgrid system and its components. (b) Schematic of the working principle of fingertip-mounted energy microgrid. Reproduced with permission from Ref. [181], © Spring Nature 2024. (c) Photographs of micropatterned holey MXene electrodes fabricated via a scalable stamping technique. (d) Demonstration of the mechanical flexibility and structural integrity of the holey MXene-based paper electrode array under bending deformation. Reproduced with permission from Ref. [182], © Spring Nature 2026. (e) Schematic illustration of anatomical positions for wearable microsensor deployment on the human body. (f) Real-time resistance response curves of the flexible sensor under varying bending angles, indicating rapid step-response characteristics. Reproduced with permission from Ref. [152], © American Chemical Society 2024. (g) Proposed interfacial adhesion mechanism between the deep eutectic solvent/ionic liquid composite gel substrate and porcine skin tissue, illustrating conformal bio-integration capability. (h) Practical demonstration of the flexible battery powering a mobile phone, highlighting potential applications in portable consumer electronics. Reproduced with permission from Ref. [185], © Wiley-VCH GmbH 2026.

density for amplified Zn^{2+} responsiveness, compressible interfaces to couple mechanical input with ionic flux, and porous conductive networks to accelerate interfacial charge transfer.

Therefore, the significance of developing a wearable AZIB sensing system lies in the integration of self-powering and self-sensing capabilities into a unified platform. This successfully establishes an intelligent system capable of continuous autonomous energy supply and real-time response to external information changes. It not only overcomes the challenge of providing long-term stable power to electronic devices in remote or extreme environments but also incorporates high-precision sensing technology.

5 Challenges and perspectives

Drawing on its inherent safety, low cost, and environmentally friendly aqueous electrolyte properties, integrated wearable AZIBs systems, through flexible structural design, can effectively conform to curved and dynamic surfaces of human body, thereby balancing wearing comfort with device reliability. From dual perspectives of energy storage and energy response, this review focuses on analyzing the working principles of wearable AZIBs integrated systems, elucidates the advantage and necessity of system integration. Further, by examining representative research cases, the review systematically explores the construction methods of such integrated systems and evaluates the effectiveness of relevant strategies in addressing their core scientific challenges.

However, wearable AZIBs integrated systems still face multidimensional and profound comprehensive challenges. At fundamental material level, the differences between energy harvesting units and battery electrode/electrolyte materials lead to inefficient energy transfer during integration. The complexity of multifunctional stacking and issues such as interfacial intricacy and stress concentration make it difficult for materials to meet high reversible response capability required for sensing functions. At device integration level, the introduction of inactive components like connecting circuits and encapsulation layers significantly compromises the system's energy and power density. Additionally, signal interference generated during battery charging/discharging and deformation processes can affect the accuracy and reliability of sensing. In terms of large-scale manufacturing, the internal structural complexity resulting from multifunctional integration imposes extremely high demands on circuit design precision and microfabrication processes. This necessitates the development of high-precision automated production lines alongside addressing environmental and safety concerns. In practical applications, the demand for continuous, all-day energy supply is challenging to meet, especially under extreme

environmental conditions. Mechanical deformation, sweat erosion, and fluctuations in temperature and humidity during daily use can easily lead to the failure of critical components. Furthermore, both safety and biocompatibility must undergo rigorous validation.

Building on the above systematic discussion, we propose the following outlook for the future development of wearable AZIBs integrated system, aiming to establish a complete technological pathway from laboratory performance breakthroughs to large-scale market application (Fig. 11).

5.1 Foundation materials

To address the issues of poor integration adaptability and insufficient stability of material interfaces under dynamic deformation in wearable AZIBs integrated system, the following core strategies can be adopted. Firstly, by constructing functionally graded composite electrodes, the energy harvesting units are coupled with zinc-ion storage active materials. Dynamic adaptive interfacial layers are employed to mitigate mechanical mismatches between different materials, thereby establishing efficient and stable ion/electron transport pathways to enhance energy transfer efficiency. Simultaneously, the introduction of intelligent polymer electrolytes with dynamic and reversible bonding capabilities ensures that the materials can maintain high reversibility in sensing responses while preserving their structural integrity during repeated deformation.

5.2 Device integration

In the integrated design of wearable AZIBs, special emphasis should be placed on dealing with challenges such as low energy supply efficiency, limited integration density, and susceptibility of sensing signals to interference under complex operating conditions. Through advancing high-density 3D heterogeneous integration technologies and ultrathin multifunctional encapsulation materials, the volume proportion of inactive components is minimized while maintaining excellent mechanical flexibility and encapsulation reliability. High-density interconnection techniques are leveraged to enhance overall energy and power density. Then embedded signal conditioning modules and adaptive noise suppression algorithms are introduced to achieve real-time isolation and compensation of sensing signals from interference caused by charging/discharging and deformation at the hardware level. Simultaneously, multimodal data fusion processing is employed to improve signal accuracy and environmental adaptability.

5.3 Scalable manufacturing

Systematic technological innovation is required to achieve high performance and scalable production of wearable AZIBs integrated system. High-precision and high-consistency integrated manufacturing of heterogeneous structures can be achieved by developing a digital production line platform with multi-process collaboration. Besides, the introduction of artificial intelligence-driven real-time process monitoring dynamically optimizes manufacturing parameters to compensate for process fluctuations, significantly improving the processing yield and performance consistency of complex structures. Additionally, it is essential to advance the development of green manufacturing processes and closed-loop material cycling systems, while establishing a comprehensive chain system covering raw materials, production, and recycling.

5.4 Practical application

To ensure the functional stability and safety of wearable AZIBs

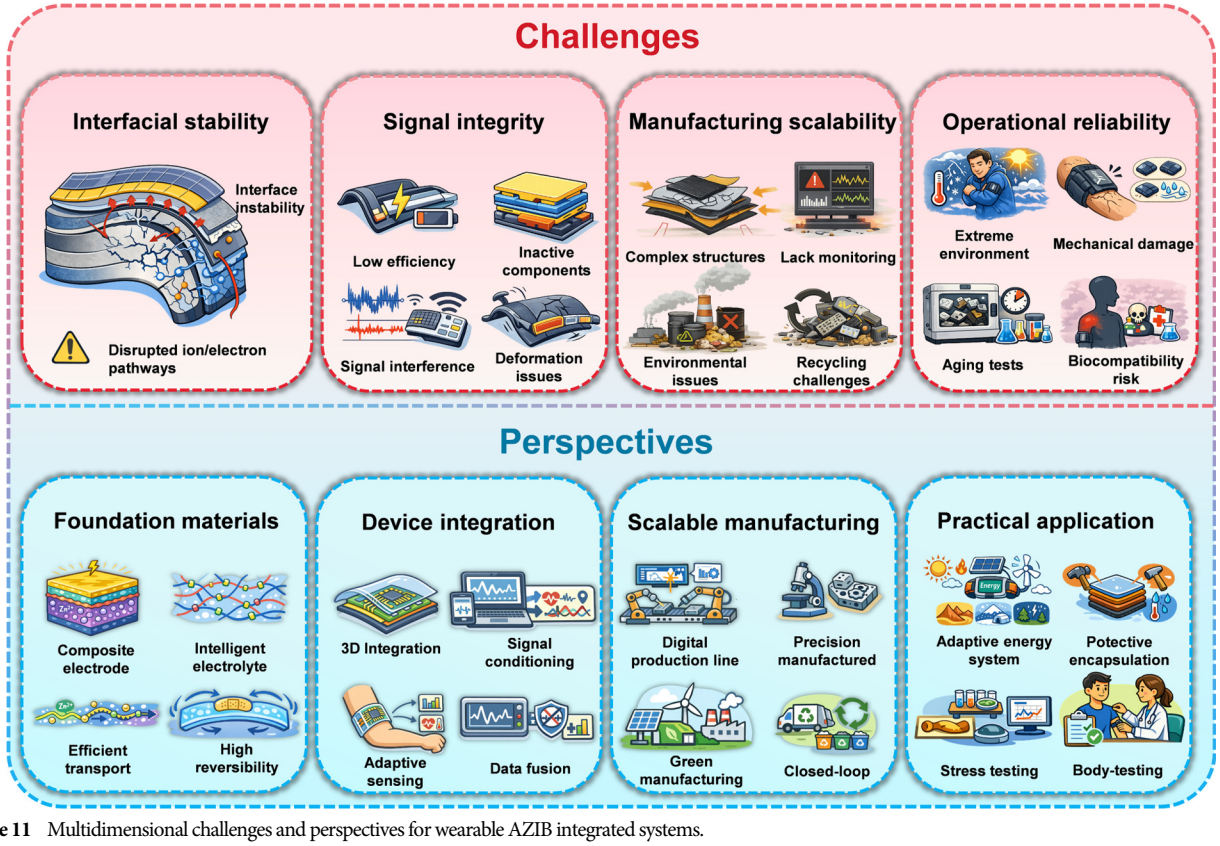

Figure 11 Multidimensional challenges and perspectives for wearable AZIB integrated systems.

integrated system in complex application scenarios, it is necessary to establish a comprehensive solution that covers environmental adaptability, structural protection, long-term verification, and biocompatibility. Environment-adaptive energy supply systems should be developed to enhance continuous operational capability under extreme conditions. Meanwhile, multi-level protective encapsulation systems should be designed to effectively resist combined threats from mechanical deformation, sweat corrosion, and temperature/humidity fluctuations. At the same time, it is essential to establish accelerated aging and failure analysis platforms to simulate the multi-stress coupling effects under real-world wearable scenarios, thereby systematically validating the long-term reliability of components. Furthermore, progress should be made step-by-step from material chemical safety and cytocompatibility to long-term human wear trials to ensure the system ultimately achieves medical compliance certification.

Guided by full-chain innovation strategy for wearable AZIBs integrated system, which spans from foundational materials to top-level system design, we would build performance foundations through material innovation, optimize ion transport via interface engineering, balance key parameters with device design, maximize overall efficiency through system integration, and ensure reliability via practical application. We are confident that this comprehensive approach will not only overcome the current technical bottlenecks of wearable AZIBs integrated system but also pave the way for their successful commercialization.

Acknowledgements

This work was supported by the Fundamental and Interdisciplinary Disciplines Breakthrough Plan of the Ministry of Education of China (JYB2025XDXM303).

Declaration of conflicting interests

The authors declare no conflicting interests regarding the content of this article.

Data availability

All data needed to support the conclusions in the paper are presented in the manuscript and/or the Supplementary Materials. Additional data related to this paper may be requested from the corresponding author upon request.

References

[1] Cao, L. Q.; Bu, F.; Wang, Y. X.; Gao, Y.; Zhao, W. B.; Yang, J. Y.; Chen, J. P.; Xu, X.; Guan, C. Multifunctional anchoring effect enables ultra-stable 3D-printed zinc powder-based anode. *Sci. China Mater.* **2025**, *68*, 897–905.

[2] Hu, X. T.; Lai, G. J.; Liu, Y. Y.; Zhou, P.; Lu, B. G.; El-Bahy, Z. M.; Ebaid, M. S.; Chen, L. N.; Zhou, J. Design of dual-electrode interfacial kinetics regulator for long-lasting Ah-level zinc-iodine batteries. *eScience* **2025**, *5*, 100455.

[3] Zheng, X. Y.; Xie, Y.; Tian, F.; Lei, D. N.; Wang, C. X. 3D porous reduced graphene cathode and non-corrosive electrolyte for long-life rechargeable aluminum batteries. *Energy Mater. Devices* **2024**, *2*, 9370032.

[4] Zhang, Y. J.; Li, M. Z.; Liang, S. Q.; Fang, G. Z. Advances on new configuration of zinc anode towards high-performance emerging zinc-based electronic devices. *Energy Mater. Devices* **2023**, *1*, 9370023.

[5] Wang, D. W.; Kong, X. Y.; Wang, Z. S.; Zhang, X. Y.; Zhang, J.; Chen, Y. H. Dual-functional Fe_3O_4-decorated porous carbon nanosheets for kinetics-enhanced aqueous zinc-iodine batteries. *Green Carbon* **2025**, *3*, 382–392.

[6] Yin, Y. B.; Li, X. F. Review and perspectives on anodes in rechargeable aqueous zinc-based batteries. *Renewables* **2023**, *1*, 622–637.

[7] Hu, X. T.; Zhao, Z. Q.; Yang, Y. Q.; Zhang, H.; Lai, G. J.; Lu, B. G.; Zhou, P.; Chen, L. N.; Zhou, J. Bifunctional self-segregated electrolyte realizing high-performance zinc-iodine batteries. *InfoMat* **2024**, *6*, e12620.

[8] Li, J. W.; Lou, Y. T.; Zhou, S.; Chen, Y. N.; Zhao, X. G.; Azizi, A.; Lin, S. Y.; Fu, L. J.; Han, C.; Su, Z. et al. Intrinsically decoupled coordination chemistries enable quasi-eutectic electrolytes with fast kinetics toward enhanced zinc-ion capacitors. *Angew. Chem.* **2024**, *136*, e202406906.

[9] Li, B.; Zeng, Y.; Zhang, W. S.; Lu, B. G.; Yang, Q.; Zhou, J.; He, Z. X. Separator designs for aqueous zinc-ion batteries. *Sci. Bull.* **2024**, *69*, 688–703.

[10] Liu, H.; Yang, M. H.; Zong, Q.; Yeh, M. H.; Chang, C. C.; Yang, L.; Huang, W. H.; Liu, C. F.; Cao, G. Z. Suppressed proton insertion enhances zinc-ion storage kinetics and stability in hydrated vanadate. *ACS Energy Lett.* **2026**, *11*, 644–653.

[11] Chen, M. J.; Gong, Y. X.; Zhao, Y. X.; Song, Y. X.; Tang, Y.; Zeng, Z. Y.; Liang, S. Q.; Zhou, P.; Lu, B. G.; Zhang, X. T. et al. Spontaneous grain refinement effect of rare earth zinc alloy anodes enables stable zinc batteries. *Natl. Sci. Rev.* **2024**, *11*, nwae205.

[12] Lv, Y. N.; Ma, Y. F.; Zhu, J. N.; Abdalla, K. K.; Wang, Y. Y.; Fan, Y. C.; Song, X.; Chang, Z.; Zhao, Y.; Sun, X. M. Regulating the conversion efficiency and kinetics of halogen-based reactions for high-performance aqueous Zn batteries. *EcoEnergy* **2025**, *3*, e70014.

[13] Li, J. W.; Zhou, S.; Meng, X. Y.; Chen, Y. N.; Fu, C. Y.; Azizi, A.; Zhao, X. G.; Xie, W. M.; Chang, Z.; Pan, A. Q. Unique ion rectifier intermediate enabled by ultrathin vermiculite sheets for high-performance Zn metal anodes. *Sci. Bull.* **2023**, *68*, 1283–1294.

[14] Liu, R. Q.; Shang, W. S.; Zhang, J. T. Bridging materials and energy storage mechanisms in Zn–I_2 batteries. *J. Electrochem.* **2025**, *31*, 2515005.

[15] Zhang, S. Y.; Gu, K. H.; Lu, B.; Han, J. W.; Zhou, J. Hydrometallurgical processes on recycling of spent lithium-ion battery cathode: Advances and applications in sustainable technologies. *Acta Phys.-Chim. Sin.* **2024**, *40*, 2309028.

[16] Zhu, J. B.; Hu, W. X.; Ni, J. F.; Li, L. Zinc micro-energy storage devices powering microsystems. *Natl. Sci. Open* **2024**, *3*, 20230078.

[17] Huang, K. X.; Zeng, X. G.; Zhang, D.; Wang, Y. J.; Lan, M.; Wen, C. Y.; Guo, Y. Tailoring crystallization zinc hydroxide sulfates growth towards stable zinc deposition chemistry. *Nano Res.* **2024**, *17*, 5243–5250.

[18] Wu, G.; Yang, W. H.; Yang, Y.; Yang, H. J. Dendrite-free strategies for aqueous zinc-ion batteries: Structure, electrolyte, and separator. *J. Electrochem.* **2024**, *30*, 2415003.

[19] Lv, W.; Liu, J. L.; Shen, Z. L.; Li, X. D.; Xu, C. Novel approaches to aqueous zinc-ion batteries: Challenges, strategies, and prospects. *eScience* **2025**, *5*, 100410.

[20] Liu, H.; Yang, L.; Shen, T.; Li, C. Y.; Kang, T.; Niu, H. H.; Huang, W. H.; Chang, C. C.; Yang, M. H.; Cao, G. Z. et al. Distorting local structures to modulate ligand fields in vanadium oxide for high-performance aqueous zinc-ion batteries. *ACS Nano* **2025**, *19*, 9132–9143.

[21] Li, H.; Yang, L.; Zhou, S.; Li, J. W.; Chen, Y. N.; Meng, X. Y.; Xu, D. M.; Han, C.; Duan, H. M.; Pan, A. Q. A self-regulated interface enabled by multi-functional pH buffer for reversible Zn electrochemistry. *Adv. Funct. Mater.* **2024**, *34*, 2313859.

[22] Zhang, Q. S.; Cui, C. Y.; Chen, H.; Pan, S. J.; Zhang, Y. H.; Zhu, J.; Lu, B. G. Surface cobaltization for boosted kinetics and excellent stability of nickel-rich layered cathodes. *Natl. Sci. Open* **2024**, *3*, 20240010.

[23] Tan, H.; Meng, C.; Sun, T.; Wu, X. L.; Liu, H.; Wang, J. J. Boosting zinc anode durability through synergistic inner Helmholtz plane and interfacial electric field regulation. *Sci. Bull.* **2024**, *69*, 2025–2029.
[24] Lv, W.; Meng, J. W.; Li, X. D.; Xu, C.; Yang, W. J.; Duan, S. Z.; Li, Y. M.; Ju, X.; Yuan, R. S.; Tian, Y. L. et al. Boosting zinc storage in potassium-birnessite via organic-inorganic electrolyte strategy with slight N-methyl-2-pyrrolidone additive. *Energy Storage Mater.* **2023**, *54*, 784–793.
[25] Meng, Z.; Jiao, Y. C.; Wu, P. Y. Alleviating side reactions on Zn anodes for aqueous batteries by a cell membrane derived phosphorylcholine zwitterionic protective layer. *Angew. Chem., Int. Ed.* **2023**, *62*, e202307271.
[26] Meng, X. Y.; Zhou, S.; Li, J. W.; Chen, Y. N.; Lin, S. Y.; Han, C.; Pan, A. Q. Regulated ion-conductive electrode-electrolyte interface by *in situ* gelation for stable zinc metal anode. *Adv. Funct. Mater.* **2024**, *34*, 2309350.
[27] Xie, X. S.; Li, J. J.; Xing, Z. Y.; Lu, B. G.; Liang, S. Q.; Zhou, J. Biocompatible zinc battery with programmable electro-cross-linked electrolyte. *Natl. Sci. Rev.* **2023**, *10*, nwac281.
[28] Liu, Z. X.; Qin, M. L.; Fu, B.; Li, M. Z.; Liang, S. Q.; Fang, G. Z. Effective proton conduction in quasi-solid zinc-manganese batteries via constructing highly connected transfer pathways. *Angew. Chem., Int. Ed.* **2025**, *64*, e202417049.
[29] Xie, Y. W.; Feng, S.; Gao, J. C.; Cheng, T.; Zhang, L. Modulating the interfacial microenvironment via zwitterionic additive for long-cycling aqueous Zn-ion batteries. *Sci. China Mater.* **2024**, *67*, 2898–2907.
[30] Lin, W. Z.; Yao, X. X.; Zhao, W.; Pu, Y. R.; Wang, S. Pathways to carbon neutrality in the built environment: Phase change materials. *Green Carbon* **2024**, *2*, 197–204.
[31] Ren, H. Z.; Zhang, J.; Wang, B.; Luo, H.; Jin, F.; Zhang, T. R.; Ding, A.; Cong, B. W.; Wang, D. L. A V_2O_3@N–C cathode material for aqueous zinc-ion batteries with boosted zinc-ion storage performance. *Rare Met.* **2022**, *41*, 1605–1615.
[32] Li, J. W.; Zhou, S.; Chen, Y. N.; Meng, X. Y.; Azizi, A.; He, Q.; Li, H.; Chen, L.; Han, C.; Pan, A. Q. Self-smoothing deposition behavior enabled by beneficial potential compensating for highly reversible Zn-metal anodes. *Adv. Funct. Mater.* **2023**, *33*, 2307201.
[33] Sun, Q.; Du, H. H.; Sun, T. J.; Li, D. T.; Cheng, M.; Liang, J.; Li, H. X.; Tao, Z. L. Sorbitol-electrolyte-additive based reversible zinc electrochemistry. *J. Electrochem.* **2024**, *30*, 2314002.
[34] Chen, M. Y.; Ma, J. J.; Feng, Y. H.; Yuan, Q. P.; Wu, Y. H.; Liu, Y. F.; Hu, G. Z.; Liu, X. J. Advancing aqueous zinc-ion batteries with carbon dots: A comprehensive review. *EcoEnergy* **2025**, *3*, 254–295.
[35] Fan, X.; Chen, L. N.; Wang, Y. J.; Xu, X. Y.; Jiao, X. X.; Zhou, P.; Liu, Y. Y.; Song, Z. X.; Zhou, J. Selection of negative charged acidic polar additives to regulate electric double layer for stable zinc ion battery. *Nano-Micro Lett.* **2024**, *16*, 270.
[36] Liu, T. T.; Lei, C. J.; Wang, H. J.; Xu, C.; Ma, W. J.; He, X.; Liang, X. Practical four-electron zinc-iodine aqueous batteries enabled by orbital hybridization induced adsorption-catalysis. *Sci. Bull.* **2024**, *69*, 1674–1685.
[37] Zhou, S.; Wang, Y. P.; Lu, H. T.; Zhang, Y. F.; Fu, C. Y.; Usman, I.; Liu, Z. X.; Feng, M. Y.; Fang, G. Z.; Cao, X. X. et al. Anti-corrosive and Zn-ion-regulating composite interlayer enabling long-life Zn metal anodes. *Adv. Funct. Mater.* **2021**, *31*, 2104361.
[38] Feng, D. D.; Jiao, Y. C.; Wu, P. Y. Proton-reservoir hydrogel electrolyte for long-term cycling Zn/PANI batteries in wide temperature range. *Angew. Chem., Int. Ed.* **2023**, *62*, e202215060.
[39] Chen, Y. N.; Zhou, S.; Li, J. W.; Kang, J. T.; Lin, S. Y.; Han, C.; Duan, H. M.; Liang, S. Q.; Pan, A. Q. Non-expendable regulator enables durable and deep cycling aqueous zinc batteries. *Adv. Energy Mater.* **2024**, *14*, 2400398.
[40] Cho, B. K.; Huh, S. H.; Kim, S. H.; Yu, S.; Bae, J. S.; Yoo, J. K.; Yu, S. H. Long cycle-life aqueous Zn battery enabled by facile carbon nanotube coating on Cu current collector. *Carbon Energy* **2024**, *6*, e441.
[41] Li, J. W.; Azizi, A.; Zhou, S.; Liu, S. N.; Han, C.; Chang, Z.; Pan, A. Q.; Cao, G. Z. Hydrogel polymer electrolytes toward better zinc-ion batteries: A comprehensive review. *eScience* **2025**, *5*, 100294.
[42] Fan, X. K.; Xiang, K. X.; Zhou, W.; Deng, W. N.; Zhu, H.; Chen, L.; Chen, H. A novel improvement strategy and a comprehensive mechanism insight for α-MnO_2 energy storage in rechargeable aqueous zinc-ion batteries. *Carbon Energy* **2024**, *6*, e536.
[43] Su, C.; Gao, X.; Liu, K. J.; Dai, Y. H.; Dong, H. B.; Liu, Y. Y.; Zhu, J. Y.; Zhang, Q. X.; He, H. Z.; He, G. J. From lab to market: A review of commercialization and advances for binders in lithium-, zinc-, sodium-ion batteries. *Nano Res. Energy* **2024**, *3*, e9120094.
[44] Zhao, C. X.; Liu, J. N.; Yao, N.; Zeng, X. Y.; Chen, A. B.; Dong, P.; Zhang, Y. J.; Ma, X. Z.; Tang, C.; Li, B. Q. et al. Low-temperature working feasibility of zinc-air batteries with noble metal-free electrocatalysts. *Renewables* **2023**, *1*, 73–80.
[45] Dou, X. Y.; Xie, X. F.; Liang, S. Q.; Fang, G. Z. Low-current-density stability of vanadium-based cathodes for aqueous zinc-ion batteries. *Sci. Bull.* **2024**, *69*, 833–845.
[46] Sun, D. F.; Wang, Z. J.; Tian, T.; Yu, X.; Yu, D. D.; Zhou, X. Z.; Ma, G. F.; Lei, Z. Q. Constructing oxygen deficiency-rich V_2O_3@PEDOT cathode for high-performance aqueous zinc-ion batteries. *Rare Met.* **2024**, *43*, 635–646.
[47] Chen, Y. N.; Zhou, S.; Li, J. W.; Zhang, X.; Zhou, C. C.; Shi, X. D.; Zhang, C. X.; Fang, G. Z.; Liang, S. Q.; Su, Z. et al. Tuning Zn^{2+} deposition kinetics towards deep-reversible zinc metal batteries with all-climate adaptability. *Angew. Chem., Int. Ed.* **2025**, *64*, e202423252.
[48] Wang, Q.; Zhou, W. H.; Zhang, Y. Y.; Jin, H. R.; Li, X. R.; Zhang, T. S.; Wang, B. Y.; Zhao, R. Z.; Zhang, J. W.; Li, W. et al. Rescue of dead MnO_2 for stable electrolytic Zn–Mn redox-flow battery: A metric of mediated and catalytic kinetics. *Natl. Sci. Rev.* **2024**, *11*, nwae230.
[49] Li, L.; Jia, S. F.; Cao, M. H.; Ji, Y. Q.; Qiu, H. W.; Zhang, D. Progress in research on metal-based materials in stabilized Zn anodes. *Rare Met.* **2024**, *43*, 20–40.
[50] Liu, G. Q.; Fu, B.; Liu, Z. X.; Li, L. Y.; Liang, S. Q.; Fang, G. Z. Copper oxide-modified highly reversible Zn powder anode for aqueous Zn metal batteries. *Rare Met.* **2024**, *43*, 5005–5016.
[51] Chen, W. J.; Tang, J. H.; Ji, F. Q.; Sun, J. L.; Zhu, Q.; Liu, B. T. A multifunctional gradient coating enables dendrite-free and side reaction-free zinc anodes for stable zinc-ion batteries. *Cell Rep. Phys. Sci.* **2023**, *4*, 101344.
[52] Shen, T.; Li, C. Y.; Wang, Y. F.; Li, Z. Q.; Yang, M. H.; Yang, L.; Liu, C. F. Fluorinated aromatic anode-electrolyte interface for highly reversible zinc anode. *Adv. Funct. Mater.* **2025**, *35*, 2509705.
[53] Song, Y. X.; Zhong, Z. Y.; Chen, M. J.; Ding, Y. Q.; Zhou, M.; Liu, Z. X.; Liang, S. Q.; Fang, G. Z. Interfacial optimization enabling reversible and stable aqueous zinc metal batteries under harsh conditions. *J. Cent. South Univ.* **2024**, *31*, 4536–4548.
[54] Sun, B. L.; Wang, N.; Xie, X. C.; Zhong, L.; He, L. X.; Komarneni, S.; Hu, W. C. Symmetrical porous graphitized carbon fabric electrodes for ultra-cryogenic and dendrite-free Zn-ion hybrid supercapacitors. *J. Mater. Sci. Technol.* **2025**, *209*, 251–261.
[55] Jiang, L.; Ding, Y. Q.; Li, L.; Tang, Y.; Zhou, P.; Lu, B. G.; Tian, S. Y.; Zhou, J. Cationic adsorption-induced microlevelling effect: A pathway to dendrite-free zinc anodes. *Nano-Micro Lett.* **2025**, *17*, 202.
[56] Zhong, Y. J.; Cao, C. C.; Zhao, L. Q.; Tadé, M. O.; Shao, Z. P. Optimization of two-dimensional solid-state electrolyte-anode interface by integrating zinc into composite anode with dual-conductive phases. *Green Carbon* **2024**, *2*, 94–100.
[57] Liu, B.; Xu, Z. B.; Wei, C.; Zhu, Z. X.; Fang, Y. Y.; Lei, X.; Zhou, Y.; Tang, C. Y.; Ni, S. Y.; Pan, H. G. et al. Re-understanding and mitigating hydrogen release chemistry toward reversible aqueous zinc metal batteries. *eScience* **2025**, *5*, 100330.
[58] Wu, L. C.; Dai, Z. Q.; Fu, H. W.; Shen, M. K.; Cha, L. M.; Lin, Y.;

Sun, F. F.; Rao, A. M.; Zhou, J.; Wen, S. C. et al. Multiple electron transfers enable high-capacity cathode through stable anionic redox. *Adv. Mater.* **2025**, *37*, 2416298.

[59] Shen, Y. F.; Fu, P. J.; Liu, J. J.; Sun, K. S.; Wen, H. Z.; Liu, P.; Lv, H.; Gu, T. T.; Yang, X. D.; Chen, L. Highly stable Zn anodes realized by 3D zincophilic and hydrophobic interphase buffer layer. *Nano Res. Energy* **2024**, *3*, e9120115.

[60] Zhao, Y. J.; Wang, Y. Y.; Li, J. Z.; Xiong, J. W.; Li, Q.; Abdalla, K. K.; Zhao, Y.; Cai, Z.; Sun, X. M. Thermodynamic and kinetic insights for manipulating aqueous Zn battery chemistry: Towards future grid-scale renewable energy storage systems. *eScience* **2025**, *5*, 100331.

[61] Liu, Y.; Feng, K. J.; Han, J. M.; Wang, F.; Xing, Y. B.; Tao, F.; Li, H. M.; Xu, B. R.; Ji, J. T.; Li, H. X. Regulation of Zn^{2+} solvation shell by a novel N-methylacetamide based eutectic electrolyte toward high-performance zinc-ion batteries. *J. Mater. Sci. Technol.* **2025**, *211*, 53–61.

[62] Sun, Q. C.; Liu, X. J.; Chang, L. H.; Lin, M.; Lu, X. G.; Cheng, H. W. Fundamental understanding of texturing electrodeposition metal zinc anodes for practical aqueous Zn-ion batteries. *EcoEnergy* **2025**, *3*, 296–320.

[63] Cheng, Y.; Jiao, Y. C.; Wu, P. Y. Manipulating Zn 002 deposition plane with zirconium ion crosslinked hydrogel electrolyte toward dendrite free Zn metal anodes. *Energy Environ. Sci.* **2023**, *16*, 4561–4571.

[64] Guo, Q.; Yang, Y.; Wang, L. R.; Chen, N.; Qu, L. T. The feasible design of quasi-solid-state aqueous tin-iodine batteries. *Renewables* **2023**, *1*, 474–483.

[65] Xu, J. X.; Ma, S. H.; Gao, P.; Guo, Y. G.; Sun, J. F.; Qiao, D. Y.; Ma, B. H.; Yuan, W. Z.; Ramakrishna, S.; Ye, T. The state-of-the-art fundamentals and applications of micro-energy systems on-chip. *Natl. Sci. Open* **2025**, *4*, 20240044.

[66] Jia, G. B.; Plentz, J.; Dellith, A.; Schmidt, C.; Dellith, J.; Schmidl, G.; Andrä, G. Biomimic vein-like transparent conducting electrodes with low sheet resistance and metal consumption. *Nano-Micro Lett.* **2020**, *12*, 19.

[67] Guan, D. Y.; Deng, Z. H.; Luo, W.; Cheng, C. J.; Wang, F. Y.; Cai, H. W.; Chen, R. X.; Wang, P.; Wu, M. Y.; Han, C. J. et al. π-d conjugated coordination mediated catalysis for four-electron-transfer fast-charging aqueous zinc-iodine batteries. *Matter* **2025**, *8*, 101932.

[68] Wang, M. M.; Ma, J. L.; Meng, Y. H.; Tong, P. Y.; Luo, R. H.; Shen, D. Y.; Zheng, X. H.; Chen, N.; Zhang, M. Y.; Song, L. et al. *In situ* formation of solid electrolyte interphase facilitates anode-free aqueous zinc battery. *eScience* **2025**, *5*, 100397.

[69] Zhang, Y.; Zou, Z. M.; Liu, Q.; Qiao, Y.; Jiang, C. H. Dual-functions of the carbon-confined oxygen on the capacitance and cycle stability enhancements of Zn-ion capacitors. *J. Mater. Sci. Technol.* **2025**, *221*, 278–288.

[70] Ge, H. Y.; Feng, X. L.; Liu, D. P.; Zhang, Y. Recent advances and perspectives for Zn-based batteries: Zn anode and electrolyte. *Nano Res. Energy* **2023**, *2*, e9120039.

[71] Lv, W.; Meng, J. W.; Li, Y. M.; Yang, W. J.; Tian, Y. L.; Lyu, X.; Duan, C. W.; Ma, X. L.; Wu, Y. Inexpensive and eco-friendly nanostructured birnessite-type δ-MnO_2: A design strategy from oxygen defect engineering and K^+ pre-intercalation. *Nano Energy* **2022**, *98*, 107274.

[72] Zhang, Q. H.; Zhang, Y. X.; Ke, L. Z.; Jiang, H. N.; Huang, Y.; Nie, Z. X.; Jin, S. Y. Biocompatible hydrogel electrolyte with high ionic conductivity and transference number towards dendrite-free Zn anodes. *J. Mater. Sci. Technol.* **2025**, *225*, 40–48.

[73] Chen, Y. N.; Hu, Y. M.; Lu, C. G.; Zhou, S.; Pan, A. Q. Thermodynamics and kinetics of aqueous zinc electrolytes in extreme temperatures: Challenges, advances, and future. *Small* **2025**, *21*, e05865.

[74] Wang, W. H.; Li, C. W.; Liu, S. Z.; Zhang, J. C.; Zhang, D. J.; Du, J. M.; Zhang, Q. C.; Yao, Y. G. Flexible quasi-solid-state aqueous zinc-ion batteries: Design principles, functionalization strategies, and applications. *Adv. Energy Mater.* **2023**, *13*, 2300250.

[75] Hu, Y. D.; Liu, Z. X.; Li, L. Y.; Guo, S.; Xie, X. F.; Luo, Z. G.; Fang, G. Z.; Liang, S. Q. Reconstructing interfacial manganese deposition for durable aqueous zinc-manganese batteries. *Natl. Sci. Rev.* **2023**, *10*, nwad220.

[76] Luo, X. P.; Shen, T.; Liu, C. F. Toward stable and safe zinc metal anodes in aqueous rechargeable batteries. *Adv. Sustain. Syst.* **2025**, *9*, e01189.

[77] Zou, Y. H.; Sun, J.; Chi, Y. L.; Cheng, X. Y.; Yang, D. J. Recent advances and challenges of cathode materials in aqueous rechargeable zinc-ion batteries. *EcoEnergy* **2024**, *2*, 599–629.

[78] Lv, W.; Shen, Z. L.; Liu, J. L.; Li, X. D.; Ding, F.; Zhang, D. Y.; Miao, L. C.; Lyu, X. F.; Li, R. J.; Wang, M. M. et al. *In situ* synthetic C encapsulated δ-MnO_2 with O vacancies: A versatile programming in bio-engineering. *Sci. Bull.* **2025**, *70*, 203–211.

[79] Lv, W.; Shen, Z. L.; Li, X. D.; Meng, J. W.; Yang, W. J.; Ding, F.; Ju, X.; Ye, F.; Li, Y. M.; Lyu, X. et al. Discovering cathodic biocompatibility for aqueous Zn–MnO_2 battery: An integrating biomass carbon strategy. *Nano-Micro Lett.* **2024**, *16*, 109.

[80] Ahn, H.; Senthil, R. A.; Jung, S.; Kumar, A.; Ubaidullah, M.; Choi, M. Y. Pulsed laser-tuned ruthenium@carbon interface for self-powered hydrogen production via zinc-hydrazine battery coupled hybrid electrolysis. *eScience* **2025**, *5*, 100408.

[81] Deng, D. J.; Ma, H. X.; Wu, S. Q.; Wang, H.; Qian, J. C.; Wu, J. C.; Li, H. M.; Yan, C.; Li, H. N.; Xu, L. Engineering electronic density and coordination environment of Mn–N_x sites via Zn cooperation for quasi-solid-state zinc-air batteries. *Renewables* **2023**, *1*, 362–372.

[82] Zhang, L.; Xiao, J.; Xiao, X. L.; Xin, W. L.; Geng, Y. H.; Yan, Z. C.; Zhu, Z. Q. Molecular engineering of self-assembled monolayers for highly utilized Zn anodes. *eScience* **2024**, *4*, 100205.

[83] Guo, S.; Qin, L. P.; Wu, J.; Liu, Z. X.; Huang, Y. H.; Xie, Y. M.; Fang, G. Z.; Liang, S. Q. Conversion-type anode chemistry with interfacial compatibility toward Ah-level near-neutral high-voltage zinc ion batteries. *Natl. Sci. Rev.* **2024**, *11*, nwae181.

[84] Huang, F.; Xu, W. H.; He, Y.; Li, D. D.; Tan, Y.; He, H. B. Electrolyte design toward high-performance zinc-iodine batteries: Progress, challenges, and prospects. *Battery Energy* **2025**, *4*, e70036.

[85] Wei, X. C.; Liang, Y. F.; Shen, H. L.; Zhao, H. Y.; Wu, J. Y.; Huang, H. F.; Liang, X. Q.; Zhou, W. Z.; Xu, S. K.; Yu, H. Z. The customization of phosphorus terminal for MXene materials by photothermal effect toward high-performance Zn-ion hybrid supercapacitors. *Battery Energy* **2025**, *4*, e70017.

[86] Zhou, L. F.; Li, J. Y.; Peng, J.; Liu, L. Y.; Zhang, H.; Wang, Y. S.; Fan, Y. M.; Wang, J. Z.; Du, T. Advanced characterization techniques for phosphate cathodes in aqueous rechargeable zinc-based batteries. *Carbon Energy* **2024**, *6*, e611.

[87] Niu, H. H.; Liu, H.; Huang, W. H.; Shen, T.; Yang, M. H.; Yeh, M. H.; Yang, L.; Liu, C. F. Enhanced working voltage in hydrated vanadate cathodes: Insights into [VO_6] octahedral distortion and V 3*d* orbital splitting. *Adv. Funct. Mater.* **2026**, *36*, e18785.

[88] Yang, M. R.; Wang, D. H.; Ling, Y. H.; Guo, X. N.; Chen, W. H. Emerging advanced photo-rechargeable batteries. *Adv. Funct. Mater.* **2024**, *34*, 2410398.

[89] Dai, Z. Q.; Chanajaree, R.; Yang, C. W.; Zhang, X. Q.; Okhawilai, M.; Pattananuwat, P.; Zhang, X. Y.; He, G. J.; Qin, J. Q. Dual-functional additives boost zinc-ion battery electrolyte over wide temperature range. *Energy Mater. Adv.* **2025**, *6*, 0139.

[90] Zhang, D.; Lu, H. F.; Duan, C. X.; Yuan, X. Y.; Zhu, Z. J.; Qin, Y.; Song, Y. H.; Jin, Y. Advances in *in situ* characterization techniques for failure mechanisms of zinc anode interfaces. *Energy Mater. Adv.* **2025**, *6*, 0141.

[91] Ma, J. D.; Liu, H.; Kang, T.; Li, C. Y.; Niu, H. H.; Yang, L.; Liu, C. F.; Cao, G. Z. Controlling ligand field of Li_3VO_4 to enhance the electrochemical performance for lithium-ion batteries. *Sci. China Mater.* **2026**, *69*, 838–847.

[92] Li, Y. T.; Lu, Z. J.; Liu, J. C.; Huang, Y. Mitigation strategies for reducing self-discharge in aqueous zinc batteries. *Device* **2025**, *3*, 100641.

[93] Wang, Z. L.; Li, Y.; Zhou, Q. N.; Li, Q. J.; Zhao, R.; Qiu, Z. X.; Zhang, R. P.; Sun, Y. F.; Wu, F.; Wu, C. et al. Multi-ion strategies toward advanced rechargeable batteries: Materials, properties, and prospects. *Energy Mater. Adv.* **2024**, *5*, 0109.

[94] Lin, Y. M.; Mou, D.; Pu, X. R.; Li, B.; Jiang, L. M.; Zhu, X. H. Piezoelectric-driven self-charging energy storage systems: From fundamental materials to emerging applications. *Mater. Today* **2025**, *86*, 414–451.

[95] Zeng, X. X.; Zhang, S.; Long, T.; Zhao, Q. Y.; Wang, H. R.; Ling, W.; Wu, X. W.; Yu, A. P.; Chen, Z. W. An amphipathic ionic sieve membrane for durable and dendrite-free zinc-ion batteries. *Renewables* **2024**, *2*, 52–60.

[96] Liu, C.; Lu, T. T.; Liang, Z. Y.; Bai, X.; Zhang, J. H.; Chang, X. Y.; Guan, L. X.; Hou, L. F.; Wei, Y. H.; Wang, Q. et al. Optimizing the interface solvation structure enables uniform zinc deposition for zinc metal batteries. *Energy Mater. Adv.* **2025**, *6*, 0161.

[97] Liu, X. L.; Xu, B. G.; Deng, S. Z.; Han, J.; An, Y. L.; Zhao, J. X.; Yang, Q. J.; Xiao, Y. N.; Fang, C. Q. Ion-sieving MXene flakes with quantum dots enable high plating capacity for dendrite-free Zn anodes. *Carbon Energy* **2024**, *6*, e603.

[98] Wang, J. Y.; Guo, W. C.; Tian, K. S.; Li, X. T.; Wang, X. Y.; Li, P. H.; Zhang, Y.; Zhang, B. S.; Zhang, B.; Liu, S. H. et al. Proof of aerobically autoxidized self-charge concept based on single catechol-enriched carbon cathode material. *Nano-Micro Lett.* **2024**, *16*, 62.

[99] Lee, H.; Lee, H.; Lee, S.; Lim, H.; Hong, S. T.; Do Kim, H.; Chae, M. S. Enhanced structural transformation enabled by low-crystalline vanadium oxides in aqueous zinc-ion batteries. *Battery Energy* **2025**, *4*, e70040.

[100] Wang, Y. Y.; Li, Q.; Xiong, J. W.; Yu, L. F.; Li, Q.; Lv, Y. N.; Abdalla, K. K.; Wang, R. Z.; Li, X. Y.; Zhao, Y. et al. High-performance vanadium oxide-based aqueous zinc batteries: Organic molecule modification, challenges, and future prospects. *EcoEnergy* **2024**, *2*, 652–678.

[101] Xu, Y. H.; Li, Z. W.; Wu, L. Y.; Dou, H.; Zhang, X. G. Solvation engineering via fluorosurfactant additive toward boosted lithium-ion thermoelectrochemical cells. *Nano-Micro Lett.* **2024**, *16*, 72.

[102] Li, L.; Liu, S. Q.; Luo, J.; Hou, X. N.; Kong, J. H.; Zhang, Q. C.; Lai, W. Y.; He, C. B. Three-dimensional architecture design enables hexaazatriphenylene-based polymers as high-voltage, long-lifespan cathodes for aqueous zinc-organic batteries. *eScience* **2025**, *5*, 100379.

[103] Hardianto, Y. P.; Mirghni, A. A.; Shah, S. S.; Alhassan, H. M.; Mohamed, M. M.; Johan, B. A.; Hakim, A. S. R.; Aziz, A. Enhanced electrochemical performance of aqueous zinc-ion batteries with porous basil-derived carbon and nanostructured MnO_2 composite cathodes. *Battery Energy* **2025**, *4*, e70024.

[104] Mo, F. N.; Liang, G. J.; Huang, Z. D.; Li, H. F.; Wang, D. H.; Zhi, C. Y. An overview of fiber-shaped batteries with a focus on multifunctionality, scalability, and technical difficulties. *Adv. Mater.* **2020**, *32*, 1902151.

[105] Niu, H. H.; Liu, H.; Yang, L.; Kang, T.; Shen, T.; Jiang, B. Q.; Huang, W. H.; Chang, C. C.; Pei, Y. Z.; Cao, G. Z. et al. Impacts of distorted local chemical coordination on electrochemical performance in hydrated vanadium pentoxide. *Nat. Commun.* **2024**, *15*, 9421.

[106] Liu, H.; Niu, H. H.; Huang, W. H.; Shen, T.; Li, C. Y.; Chang, C. C.; Yang, M. H.; Gao, C. L.; Yang, L.; Zong, Q. et al. Unveiling the local structure and the ligand field of organic cation preintercalated vanadate cathode for aqueous zinc-ion batteries. *ACS Energy Lett.* **2024**, *9*, 5492–5501.

[107] Ding, B. B.; Tang, J. H.; Wang, Z. Q.; Liu, Z.; Xia, H. Y.; Wang, S.; Li, C. L.; Zhang, Y.; Jia, H.; Zheng, X. H. A high-capacity yarn-shaped Zn–MnO_2 battery for wearable electronics. *Colloids Surf. A: Physicochem. Eng. Aspects* **2025**, *711*, 136357.

[108] Boruah, B. D.; Mathieson, A.; Wen, B.; Feldmann, S.; Dose, W. M.; De Volder, M. Photo-rechargeable zinc-ion batteries. *Energy Environ. Sci.* **2020**, *13*, 2414–2421.

[109] Chen, P.; Li, T. T.; Yang, Y. B.; Li, G. R.; Gao, X. P. Coupling aqueous zinc batteries and perovskite solar cells for simultaneous energy harvest, conversion and storage. *Nat. Commun.* **2022**, *13*, 64.

[110] Xia, Z.; Li, S.; Wu, G. Q.; Shao, Y. Y.; Yang, D. Z.; Luo, J. R.; Jiao, Z. Y.; Sun, J. Y.; Shao, Y. L. Manipulating hierarchical orientation of wet-spun hybrid fibers via rheological engineering for Zn-ion fiber batteries. *Adv. Mater.* **2022**, *34*, 2203905.

[111] He, J. Q.; Lu, C. H.; Jiang, H. B.; Han, F.; Shi, X.; Wu, J. X.; Wang, L. Y.; Chen, T. Q.; Wang, J. J.; Zhang, Y. et al. Scalable production of high-performing woven lithium-ion fibre batteries. *Nature* **2021**, *597*, 57–63.

[112] Li, H. F.; Liu, Z. X.; Liang, G. J.; Huang, Y.; Huang, Y.; Zhu, M. S.; Pei, Z. X.; Xue, Q.; Tang, Z. J.; Wang, Y. K. et al. Waterproof and tailorable elastic rechargeable yarn zinc ion batteries by a cross-linked polyacrylamide electrolyte. *ACS Nano* **2018**, *12*, 3140–3148.

[113] Wang, C. F.; He, T.; Cheng, J. L.; Guan, Q.; Wang, B. Bioinspired interface design of sewable, weavable, and washable fiber zinc batteries for wearable power textiles. *Adv. Funct. Mater.* **2020**, *30*, 2004430.

[114] Wang, Y. B.; Li, Q.; Hong, H.; Yang, S.; Zhang, R.; Wang, X. Q.; Jin, X.; Xiong, B.; Bai, S. C.; Zhi, C. Y. Lean-water hydrogel electrolyte for zinc ion batteries. *Nat. Commun.* **2023**, *14*, 3890.

[115] Li, G. J.; Zhao, Z. H.; Zhang, S. L.; Sun, L.; Li, M. N.; Yuwono, J. A.; Mao, J. F.; Hao, J. N.; Vongsvivut, J.; Xing, L. D. et al. A biocompatible electrolyte enables highly reversible Zn anode for zinc ion battery. *Nat. Commun.* **2023**, *14*, 6526.

[116] Nguyen, T. N.; Iranpour, B.; Cheng, E.; Madden, J. D. W. Washable and stretchable Zn–MnO_2 rechargeable cell. *Adv. Energy Mater.* **2022**, *12*, 2103148.

[117] Cao, Q. H.; Gao, Y.; Pu, J.; Zhao, X.; Wang, Y. X.; Chen, J. P.; Guan, C. Gradient design of imprinted anode for stable Zn-ion batteries. *Nat. Commun.* **2023**, *14*, 641.

[118] Huang, S. W.; Hou, L.; Li, T. Y.; Jiao, Y. C.; Wu, P. Y. Antifreezing hydrogel electrolyte with ternary hydrogen bonding for high-performance zinc-ion batteries. *Adv. Mater.* **2022**, *34*, 2110140.

[119] Feng, D. D.; Xie, Y. C.; Jiao, Y. C.; Wu, P. Y. Leveraging cation effect for low temperature aqueous Zn-based batteries. *Nat. Commun.* **2025**, *16*, 9254.

[120] Wen, Z.; Yeh, M. H.; Guo, H. Y.; Wang, J.; Zi, Y. L.; Xu, W. D.; Deng, J. N.; Zhu, L.; Wang, X.; Hu, C. G. et al. Self-powered textile for wearable electronics by hybridizing fiber-shaped nanogenerators, solar cells, and supercapacitors. *Sci. Adv.* **2016**, *2*, e1600097.

[121] Lin, Y.; Huang, J.; Wang, S. J.; Qi, L. H.; Chen, W. M.; Yu, L.; Chen, C. J. Stretchable, adhesive, anti-freezing hydrogel electrolytes with dual-functional water regulation enabled by amide group-salt-water interactions for all-climate zinc-ion batteries. *Adv. Mater.* **2025**, *37*, e09975.

[122] Yao, M. J.; Yuan, Z. S.; Li, S. S.; He, T. W.; Wang, R.; Yuan, M. J.; Niu, Z. Q. Scalable assembly of flexible ultrathin all-in-one zinc-ion batteries with highly stretchable, editable, and customizable functions. *Adv. Mater.* **2021**, *33*, 2008140.

[123] Yang, P. H.; Li, J.; Lee, S. W.; Fan, H. J. Printed zinc paper batteries. *Adv. Sci.* **2022**, *9*, 2103894.

[124] Xie, C.; Guo, Y. P.; Zheng, Z. J. Pushing the limit of flexible batteries. *CCS Chem.* **2023**, *5*, 531–543.

[125] Yang, C. W.; Woottapanit, P.; Geng, S. N.; Chanajaree, R.; Shen, Y.; Lolupiman, K.; Limphirat, W.; Pakornchote, T.; Bovornratanaraks, T.; Zhang, X. Y. et al. A multifunctional quasi-solid-state polymer electrolyte with highly selective ion highways for practical zinc ion batteries. *Nat. Commun.* **2025**, *16*, 183.

[126] Shen, Z. X.; Zhai, Z. C.; Liu, Y.; Bao, X. W.; Zhu, Y. C.; Zhang, T.; Li, L. S.; Hong, G.; Zhang, N. Hydrogel electrolytes-based rechargeable zinc-ion batteries under harsh conditions. *Nano-Micro Lett.* **2025**, *17*, 227.

[127] Ma, D. T.; Li, F.; Ouyang, K. F.; Chen, Q. T.; Zhao, J. L.; Chen, M. F.; Yang, M.; Wang, Y. Y.; Chen, J. Z.; Mi, H. W. et al. An electrochemically driven hybrid interphase enabling stable versatile zinc metal electrodes for aqueous zinc batteries. *Nat. Commun.* **2025**, *16*, 4817.

[128] Shinde, S. S.; Wagh, N. K.; Lee, C. H.; Kim, D. H.; Kim, S. H.; Um, H. D.; Lee, S. U.; Lee, J. H. Scaling-up insights for zinc-air battery technologies realizing reversible zinc anodes. *Adv. Mater.* **2023**, *35*, 2303509.
[129] Dong, H. B.; Li, J. W.; Guo, J.; Lai, F. L.; Zhao, F. J.; Jiao, Y. D.; Brett, D. J. L.; Liu, T. X.; He, G. J.; Parkin, I. P. Insights on flexible zinc-ion batteries from lab research to commercialization. *Adv. Mater.* **2021**, *33*, 2007548.
[130] Hao, J. N.; Qiao, S. Z. High-voltage aqueous zinc-ion batteries with conversion-type anode and modified electrolyte. *Natl. Sci. Rev.* **2024**, *11*, nwae229.
[131] Yin, L.; Scharf, J.; Ma, J.; Doux, J. M.; Redquest, C.; Le, V. L.; Yin, Y. J.; Ortega, J.; Wei, X.; Wang, J. et al. High performance printed AgO–Zn rechargeable battery for flexible electronics. *Joule* **2021**, *5*, 228–248.
[132] Jian, R. D.; Mashhadian, A.; Wang, C. X.; Hwang, T.; Hao, Y.; Cho, K.; Xiong, G. P. Reassessing the commercialization of aqueous zinc-ion batteries based on laboratory achievements. *ACS Appl. Energy Mater.* **2025**, *8*, 12460–12479.
[133] Chen, F.; Li, X.; Chen, S. P.; Zhang, Y. L.; Huang, H. D.; Yang, H. L.; Zhou, S. Y.; Li, Z. M. Tough cellulose hydrogel electrolyte with low solvation for highly reversible and flexible aqueous zinc-ion battery. *Adv. Sci.* **2025**, *12*, e11759.
[134] Huang, S.; Wan, F.; Bi, S. S.; Zhu, J. C.; Niu, Z. Q.; Chen, J. A self-healing integrated all-in-one zinc-ion battery. *Angew. Chem., Int. Ed.* **2019**, *58*, 4313–4317.
[135] Zamarayeva, A. M.; Ostfeld, A. E.; Wang, M.; Duey, J. K.; Deckman, I.; Lechêne, B. P.; Davies, G.; Steingart, D. A.; Arias, A. C. Flexible and stretchable power sources for wearable electronics. *Sci. Adv.* **2017**, *3*, e1602051.
[136] Liepold, H.; Bird, A.; Heizmann, P. A.; Fadlullah, H.; Nguyen, H.; Klose, C.; Holdcroft, S.; Kusoglu, A.; Vierrath, S.; Münchinger, A. High protonic resistance of hydrocarbon-based cathodes in PEM fuel cells under low humidity conditions: Origin, implication, and mitigation. *J. Power Sources* **2024**, *624*, 235537.
[137] Cai, Q. Q.; Di, G. R.; Yin, X. J.; Liu, Y.; Wang, G. Q.; Kuang, Y. B.; Xiang, X. Q.; Wang, K. X.; Zhang, L.; Chen, X. et al. The photoelectrode of photo-rechargeable zinc-ion batteries: Design, progress. *J. Power Sources* **2025**, *628*, 235854.
[138] Zhao, J. Q.; Xu, Z. J.; Zhou, Z.; Xi, S. B.; Xia, Y. P.; Zhang, Q. Y.; Huang, L. Q.; Mei, L.; Jiang, Y.; Gao, J. W. et al. A safe flexible self-powered wristband system by integrating defective MnO_{2-x} nanosheet-based zinc-ion batteries with perovskite solar cells. *ACS Nano* **2021**, *15*, 10597–10608.
[139] Ruppert, J.; Stegemann, L.; Bauer, A.; Bieker, P.; Grünebaum, M.; Tempel, H.; Windmüller, A.; Leker, J.; Winter, M.; Eichel, R. A. et al. Competitive rechargeable zinc batteries for energy storage. *Adv. Energy Mater.* **2025**, *15*, e02866.
[140] Chen, M.; Guo, X.; Farhadi, B.; Guo, X. J.; Zhu, Y.; Zhou, C.; Li, X. D.; Wang, K.; Yang, D.; Jiang, X. et al. Highest overall conversion efficiency for portable thin-film zinc-ion batteries photorecharged by flexible perovskite solar cells. *Chem. Eng. J.* **2025**, *518*, 164711.
[141] Jin, K. J.; Yu, Y. J. Principles, progress, and prospects of photo-rechargeable zinc-ion batteries. *J. Energy Chem.* **2025**, *104*, 382–396.
[142] Gourley, S. W. D.; Brown, R.; Adams, B. D.; Higgins, D. Zinc-ion batteries for stationary energy storage. *Joule* **2023**, *7*, 1415–1436.
[143] Yu, X. Y.; Li, Z. G.; Wu, X. H.; Zhang, H. T.; Zhao, Q. G.; Liang, H. F.; Wang, H.; Chao, D. L.; Wang, F.; Qiao, Y. et al. Ten concerns of Zn metal anode for rechargeable aqueous zinc batteries. *Joule* **2023**, *7*, 1145–1175.
[144] Tang, L.; Peng, H. J.; Kang, J. R.; Chen, H.; Zhang, M. Y.; Liu, Y.; Kim, D. H.; Liu, Y. J.; Lin, Z. Q. Zn-based batteries for sustainable energy storage: Strategies and mechanisms. *Chem. Soc. Rev.* **2024**, *53*, 4877–4925.
[145] Wang, Z. F.; Ruan, Z. H.; Ng, W. S.; Li, H. F.; Tang, Z. J.; Liu, Z. X.; Wang, Y. K.; Hu, H.; Zhi, C. Y. Integrating a triboelectric nanogenerator and a zinc-ion battery on a designed flexible 3D spacer fabric. *Small Methods* **2018**, *2*, 1800150.
[146] Ge, Y.; Peng, L.; Cao, X.; Wang, N. Triboelectrically active hydrogel drives self-charging zinc-ion battery and human motion sensing. *Nano Energy* **2024**, *126*, 109601.
[147] Wang, H.; Zhao, B.; Li, W. X.; Liu, Y. M.; Li, L.; Zhao, Y. W.; Zhang, W. M. Piezoelectric-induced piezo ionic effect enabling high-performance flexible sensors and batteries for intelligent target shooting training. *Chem. Eng. J.* **2025**, *512*, 162523.
[148] Zhao, Y. W.; Zhu, J. X.; Lv, H. M.; Zhi, C. Y. Aqueous zinc-based batteries are flexible, self-healing, self-charging, biocompatible, and biodegradable. *Device* **2024**, *2*, 100556.
[149] Wu, H. Y.; Shan, C. C.; Fu, S. K.; Li, K. X.; Wang, J.; Xu, S. Y.; Li, G.; Zhao, Q. H.; Guo, H. Y.; Hu, C. G. Efficient energy conversion mechanism and energy storage strategy for triboelectric nanogenerators. *Nat. Commun.* **2024**, *15*, 6558.
[150] Li, Y.; Yang, W.; Han, L.; Li, H. J.; Wen, Z. G.; Li, Y.; Wang, X. G.; Sun, H. C.; Lu, T.; Xu, M.; Pan, L. K. Recent progress and perspective of multifunctional integrated zinc-ion supercapacitors. *Energy Mater.* **2022**, *2*, 200018.
[151] Castro-Rojas, J.; Rao, M. A.; Berruti, I.; Mora, M. L.; Garrido-Ramírez, E.; Polo-López, M. I. Assessment of solar photocatalytic wastewater disinfection and microcontaminants removal by modified-allophane nanoclays based on TiO_2, Fe and ZnO at laboratory and pilot scale. *Chem. Eng. J.* **2025**, *503*, 157894.
[152] Wang, Z. Q.; Xue, R. R.; Zhang, H. Q.; Zhang, Y. C.; Tang, X. Y.; Wang, H. L.; Shao, A. H.; Ma, Y. A hydrogel electrolyte toward a flexible zinc-ion battery and multifunctional health monitoring electronics. *ACS Nano* **2024**, *18*, 7596–7609.
[153] Hu, Y. P.; Liu, K. Y.; Bai, R. N.; Liu, D. Z.; Yu, W.; Meng, C. Z.; Li, G. X.; Guo, S. J. Rechargeable self-powered pressure sensor based on Zn-ion battery with high sensitivity and broad-range response. *Chem. Eng. J.* **2024**, *497*, 154812.
[154] Kao, C. C.; Ye, C.; Hao, J. N.; Chen, Y. J.; Zhang, S. J.; Qiao, S. Z. Achieving high energy density in aqueous zinc-ion batteries. *Adv. Energy Mater.* **2025**, *15*, 2501201.
[155] Chen, S. Y.; Wang, Y. H.; Fan, S. S.; Lang, X. M.; Li, G. Intriguing phenomenon of hydrogen molecules occupancy in clathrate hydrate cages: Implications for hydrogen storage. *Chem. Eng. J.* **2024**, *499*, 156089.
[156] Jia, P. X.; Zhang, Q. X.; Ren, Z. Q.; Yin, J. Y.; Lei, D. D.; Lu, W. Z.; Yao, Q. Q.; Deng, M. F.; Gao, Y. H.; Liu, N. S. Self-powered flexible battery pressure sensor based on gelatin. *Chem. Eng. J.* **2024**, *479*, 147586.
[157] Han, D. Y.; Song, C. K.; Lee, G.; Song, W. J.; Park, S. A comprehensive review of battery-integrated energy harvesting systems. *Adv. Mater. Technol.* **2024**, *9*, 2302236.
[158] Deka Boruah, B.; Mathieson, A.; Park, S. K.; Zhang, X.; Wen, B.; Tan, L. F.; Boies, A.; De Volder, M. Vanadium dioxide cathodes for high-rate photo-rechargeable zinc-ion batteries. *Adv. Energy Mater.* **2021**, *11*, 2100115.
[159] Zhu, J. Q.; Wu, H.; Li, X.; Li, M. Y.; Li, Z. L.; Xu, X. F.; Gu, L. H.; Yin, D. X.; Shen, F.; Huang, D. S. et al. Hydrogel crosslinked with nanoparticles for prevention of surgical hemorrhage and recurrence of hepatocellular carcinoma. *Adv. Sci.* **2024**, *11*, 2305508.
[160] Ullah, B.; Wang, T. Y.; Cai, R. M.; Feng, Y. H.; Ming, X. Q.; Hassanzadeh-Aghdam, M. K.; Zeng, L. Y.; Xi, K.; Tian, L.; Shen, G. Z. Design principles of flexible substrates and polymer electrolytes for flexible zinc ion batteries. *Small* **2025**, *21*, 2501671.
[161] Liu, Q.; Yu, Z. L.; Zhuang, Q. N.; Kim, J. K.; Kang, F. Y.; Zhang, B. Anti-fatigue hydrogel electrolyte for all-flexible Zn-ion batteries. *Adv. Mater.* **2023**, *35*, 2300498.
[162] Chen, Z. J.; Shen, T. Y.; Xiao, X.; He, X. C.; Luo, Y. L.; Jin, Z.; Li, C. H. An ultrahigh-modulus hydrogel electrolyte for dendrite-free zinc ion batteries. *Adv. Mater.* **2024**, *36*, 2413268.
[163] Mondal, S.; Thakur, S.; Maiti, S.; Bhattacharjee, S.; Chattopadhyay, K. K. Self-charging piezo-supercapacitor: One-step mechanical energy conversion and storage. *ACS Appl. Mater. Interfaces* **2023**, *15*, 8446–8461.
[164] Gong, Z. L.; Kong, D. X.; Chen, N.; Zhang, F. L.; Wang, D. D.;

Qian, Z.; Yang, J. Theoretical insights into aqueous zinc metal batteries: Applications of density functional theory and molecular dynamics simulations in electrolyte design. *Adv. Funct. Mater.* **2026**, *36*, e13415.
[165] Zhang, Q. X.; Lei, D. D.; Liu, N. S.; Liu, Z. Y.; Ren, Z. Q.; Yin, J. Y.; Jia, P. X.; Lu, W. Z.; Gao, Y. H. A zinc-ion battery-type self-powered pressure sensor with long service life. *Adv. Mater.* **2022**, *34*, 2205369.
[166] Wang, T.; Xi, Q.; Yao, K.; Liu, Y. H.; Fu, H.; Kavarthapu, V. S.; Lee, J. K.; Tang, S. C.; Fattakhova-Rohlfing, D.; Ai, W. et al. Surface patterning of metal zinc electrode with an in-region zincophilic interface for high-rate and long-cycle-life zinc metal anode. *Nano-Micro Lett.* **2024**, *16*, 112.
[167] Li, B.; Zhang, X. T.; Wang, T. T.; He, Z. X.; Lu, B. G.; Liang, S. Q.; Zhou, J. Interfacial engineering strategy for high-performance Zn metal anodes. *Nano-Micro Lett.* **2022**, *14*, 6.
[168] Zhao, Y. W.; Li, X.; Hou, N. L.; Yuan, T.; Huang, S. H.; Li, L.; Li, X. T.; Zhang, W. M. Self-powered sensor integration system based on thorn-like polyaniline composites for smart home applications. *Nano Energy* **2022**, *104*, 107966.
[169] Pan, J.; Liu, Y. H.; Yang, J.; Wu, J. W.; Fan, H. J. Bio-catalyzed oxidation self-charging zinc-polymer batteries. *Proc. Natl. Acad. Sci. USA* **2024**, *121*, e2312870121.
[170] Paudel, A.; Crum, A. N.; Wang, Y. Self-charging zinc-ion battery using a piezoelectric separator immersed in a hydrogel electrolyte. *ACS Appl. Mater. Interfaces* **2024**, *16*, 57130–57140.
[171] Du, M. Z.; Liu, W.; Liu, N.; Ling, Y.; Kang, S. F. Mechanisms of noble metal-enhanced ferroelectric spontaneous polarized photocatalysis. *Nano Energy* **2024**, *124*, 109495.
[172] Sun, M.; Ji, G. C.; Li, M. Z.; Zheng, J. P. A robust hydrogel electrolyte with ultrahigh ion transference number derived from zincophilic "chain-gear" network structure for dendrite-free aqueous zinc ion battery. *Adv. Funct. Mater.* **2024**, *34*, 2402004.
[173] Huang, Y.; Liu, B. B.; Zhang, W. Y.; Qu, G. R.; Jin, S. Y.; Li, X. B.; Nie, Z. X.; Zhou, H. Highly sensitive active-powering pressure sensor enabled by integration of double-rough surface hydrogel and flexible batteries. *npj Flex. Electron.* **2022**, *6*, 92.
[174] Li, Y. Q.; Miao, R. T.; Yang, Y.; Han, L.; Han, Q. S. A zinc-ion battery-type self-powered strain sensing system by using a high-performance ionic hydrogel. *Soft Matter* **2023**, *19*, 8022–8032.
[175] Shi, M. Y.; Zhang, J. L.; Tang, G. C.; Wang, B.; Wang, S.; Ren, X. X.; Li, G. J.; Chen, W. H.; Liu, C. T.; Shen, C. Y. Polyzwitterionic cross-linked double network hydrogel electrolyte enabling high-stable Zn anode. *Nano Res.* **2024**, *17*, 5278–5287.
[176] Chen, J. Z.; Chen, M. F.; Chen, H. L.; Yang, M.; Han, X.; Ma, D. T.; Zhang, P. X.; Wong, C. P. Wood-inspired anisotropic hydrogel electrolyte with large modulus and low tortuosity realizing durable dendrite-free zinc-ion batteries. *Proc. Natl. Acad. Sci. USA* **2024**, *121*, e2322944121.
[177] Li, Y. Q.; Yang, Y.; Liu, X. H.; Yang, Y. W.; Wu, Y. Y.; Han, L.; Han, Q. S. Flexible self-powered integrated sensing system based on a rechargeable zinc-ion battery by using a multifunctional polyacrylamide/carboxymethyl chitosan/LiCl ionic hydrogel. *Colloids Surf. A: Physicochem. Eng. Aspects* **2022**, *648*, 129254.
[178] Lu, D. J.; Hao, Y. C.; Wang, Z. Q.; He, J.; Huang, X. J.; Shi, Y. X.; Gao, S.; Zhang, H. Q.; Ma, Y.; Xu, F. et al. Zn–PAA–C hydrogel for integrated energy storage and self-diagnostic health monitoring in wearable biomedical devices. *Energy Storage Mater.* **2025**, *80*, 104407.
[179] Du, X. Y.; Song, L. N.; Liang, S.; Wang, Y. F.; Wang, Y.; Wang, H. F.; Xu, J. J. Photo-assisted chemical self-rechargeable zinc ion batteries with high charging and discharging efficiency. *Angew. Chem., Int. Ed.* **2024**, *63*, e202411845.
[180] Zhang, B. Y.; Cai, X. Z.; Li, J. J.; Zhang, H.; Li, D. M.; Ge, H. Y.; Liang, S. Q.; Lu, B. G.; Zhao, J. Q.; Zhou, J. Biocompatible and stable quasi-solid-state zinc-ion batteries for real-time responsive wireless wearable electronics. *Energy Environ. Sci.* **2024**, *17*, 3878–3887.
[181] Ding, S. C.; Saha, T.; Yin, L.; Liu, R. X.; Khan, M. I.; Chang, A. Y.; Lee, H.; Zhao, H.; Liu, Y. Z.; Nazemi, A. S. et al. A fingertip-wearable microgrid system for autonomous energy management and metabolic monitoring. *Nat. Electron.* **2024**, *7*, 788–799.
[182] Wang, M. J.; Chen, C.; Zhang, Y. H.; Ma, Y. N.; Xu, L.; Wu, D. D.; Gao, B. W.; Song, A. Y.; Wen, L.; Cheng, Y. F. et al. Flexible monolithic 3D-integrated self-powered tactile sensing array based on holey MXene paste. *Nano-Micro Lett.* **2026**, *18*, 68.
[183] Ma, N.; Liu, M. Y.; Liu, Z. Y.; Cai, Z. Z.; Yan, S. W.; Wang, F.; Zhang, J. S.; Ma, L.; Gao, Y. H.; Cheng, Y. F. et al. Human motion and posture classification with self-powered MXene-zinc ion pressure sensor. *Device* **2025**, *3*, 100937.
[184] Zhang, X. S.; Jia, C. E.; Zhang, J. Y.; Zhang, L. L.; Liu, X. Y. Smart aqueous zinc ion battery: Operation principles and design strategy. *Adv. Sci.* **2024**, *11*, 2305201.
[185] Li, T.; Liu, J. T.; Shu, H.; Sun, A. K.; Zhao, T.; Chen, Y.; Chen, Y. High-performance deep eutectic/ionic liquid gels for zinc-ion battery and flexible sensor applications in extreme environments. *Adv. Funct. Mater.* **2026**, *36*, e14358.

Wei Lv received his Ph.D. degree from Central Iron & Steel Research Institute. He is currently an associate professor at North China Electric Power University. His research interest mainly includes the application of aqueous batteries.

Chao Xu received his Ph.D. degree from The Hong Kong University of Science and Technology. Presently, he is a professor at North China Electric Power University. His research covers a wide area including advanced energy storage and renewable power generation.